

## Emerging chemistries and molecular designs for flow batteries

Leyuan Zhang<sup>1,2</sup>, Ruozhu Feng<sup>3</sup>, Wei Wang<sup>3</sup>  and Guihua Yu<sup>1,2</sup> 

**Abstract** | Redox flow batteries are a critical technology for large-scale energy storage, offering the promising characteristics of high scalability, design flexibility and decoupled energy and power. In recent years, they have attracted extensive research interest, with significant advances in relevant materials chemistry, performance metrics and characterization. The emerging concepts of hybrid battery design, redox-targeting strategy, photoelectrode integration and organic redox-active materials present new chemistries for cost-effective and sustainable energy storage systems. This Review summarizes the recent development of next-generation redox flow batteries, providing a critical overview of the emerging redox chemistries of active materials from inorganics to organics. We discuss electrochemical characterizations and critical performance assessment considering the intrinsic properties of the active materials and the mechanisms that lead to degradation of energy storage capacity. In particular, we highlight the importance of advanced spectroscopic analysis and computational studies in enabling understanding of relevant mechanisms. We also outline the technical requirements for rational design of innovative materials and electrolytes to stimulate more exciting research and present the prospect of this field from aspects of both fundamental science and practical applications.

With increasing concerns about energy security and environmental issues globally, there has been an increased focus on the move away from fossil-fuel-based energy sources. As a consequence, there have also been significant changes in the energy storage landscape over the past few years<sup>1</sup>. The development of energy storage technologies has enabled, for example, increased market penetration of electric vehicles, with profound impacts on the power grid<sup>2</sup>. The desire to develop a green and sustainable society and lifestyle has meant that renewable energy sources have made up an increasingly large share of energy consumption. However, the efficient use of renewable energy requires low-cost and long-life energy storage to incorporate it into the traditional grid system<sup>3–5</sup>. In the USA in 2021, the new administration called for greater efforts to accelerate innovations in affordable long-duration energy storage, as this is an essential component of the long-term goal of decarbonizing the US power sector by 2035 and development of a net-zero emissions economy by 2050. Similar moves have been made worldwide<sup>6–8</sup>. While lithium-ion batteries have been successfully deployed for portable electronics and electric vehicles, the relatively high energy cost and limited ability to decouple power and energy could render that technology uneconomical for long-duration energy storage needed for deep decarbonization<sup>2</sup>.

By comparison, redox flow battery (RFB) technology is one of the most promising alternatives for grid-scale energy storage with high scalability and decoupled energy and power<sup>9</sup>. Decoupling refers to the ability to have independent control of energy storage and power output by scaling up the electrolyte storage tanks and the electrodes, respectively, which is difficult to implement for rechargeable metal-ion batteries. However, the widespread application of traditional flow batteries is restricted by the requirement for low-abundance redox-active metals combined with environmental concerns, high cost and relatively low energy density<sup>10</sup>. Recently, new materials chemistry has attracted extensive interest for next-generation RFB development. This Review provides a critical overview of recent progress in next-generation flow batteries, highlighting the latest innovative materials and chemistries. We outline the assessment methods, advanced characterization and technical requirements for the development of practical RFBs, and the remaining challenges that need to be addressed, and we provide our view of promising future research directions.

### Flow battery system classification

Flow batteries were first proposed in the early 1880s and have since undergone many developments<sup>11</sup>. FIGURE 1a illustrates the general configuration of conventional

<sup>1</sup>Materials Science and Engineering Program, The University of Texas at Austin, Austin, TX, USA.

<sup>2</sup>Walker Department of Mechanical Engineering, The University of Texas at Austin, Austin, TX, USA.

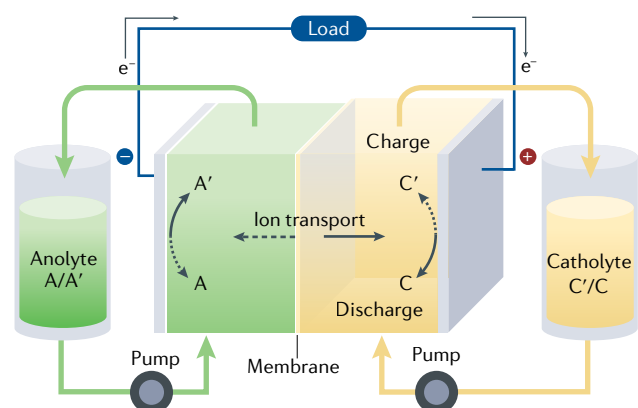
<sup>3</sup>Pacific Northwest National Laboratory, Richland, WA, USA.

✉e-mail: [wei.wang@pnnl.gov](mailto:wei.wang@pnnl.gov); [ghyu@austin.utexas.edu](mailto:ghyu@austin.utexas.edu)  
<https://doi.org/10.1038/s41570-022-00394-6>

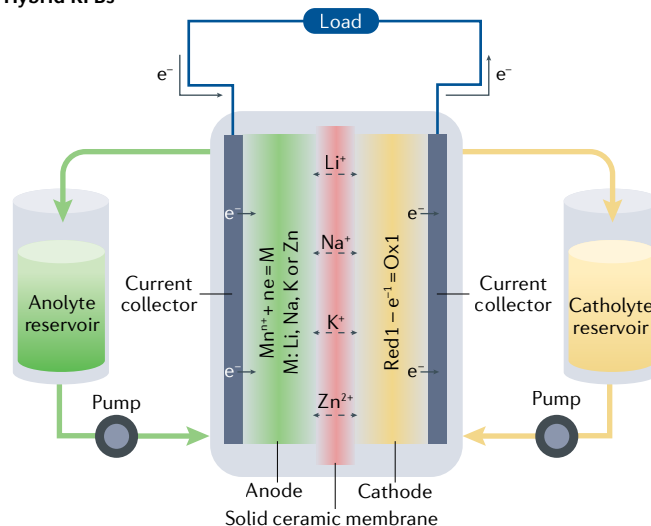
RFBs and basic working principles. RFBs work in a distinctly different fashion to Li-ion batteries. In RFBs, the energy-bearing redox-active materials are generally

dissolved in flowing electrolytes to fulfil the conversion of chemical and electrical energies. In the cell stack, negative and positive electrolytes, referred to as the

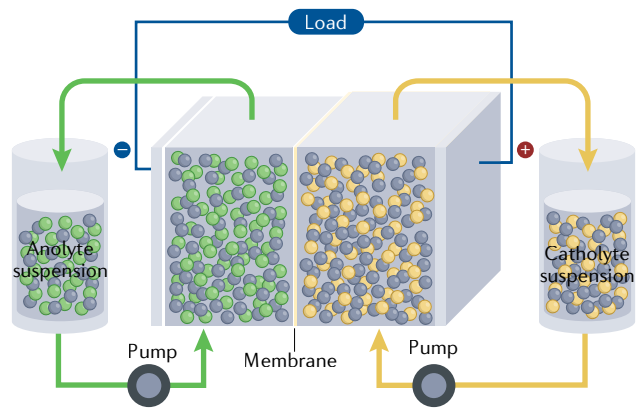
**a Traditional RFBs**



**b Hybrid RFBs**



**c Semi-solid RFBs**



**d Solar RFBs**

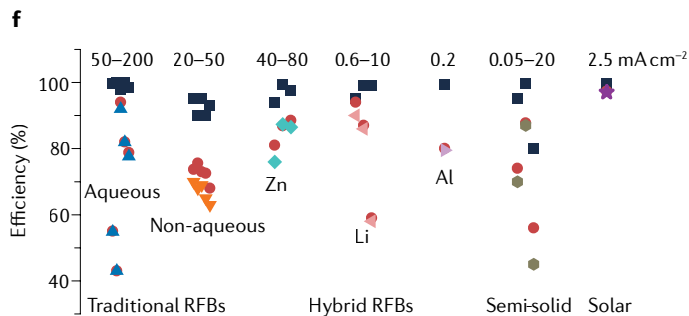
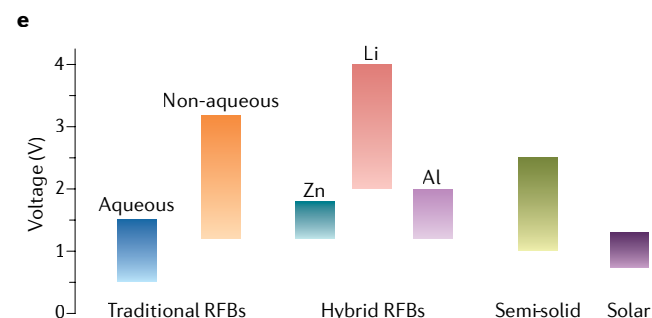
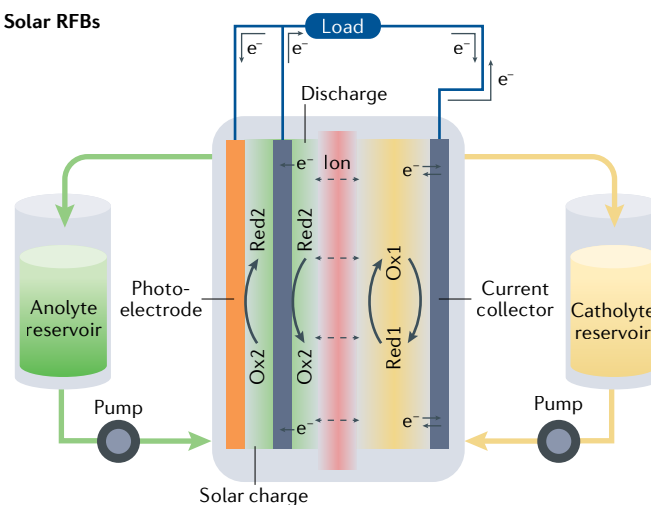


**Fig. 1 | Development of important flow battery types. a** | A typical redox flow battery (RFB) with redox-active materials dissolved in liquid electrolytes. Electrolytes flow through current collectors and redox reactions occur at the electrolyte–electrode interface. When discharging, redox species in catholyte are reduced, while those in the anolyte are oxidized; charge carriers are transported through the membrane from anolyte to catholyte to maintain neutrality. **b** | A hybrid flow battery with different metal anodes (lithium, sodium, potassium or zinc) and appropriate catholytes, in which solid ceramic or polymer (Nafion) membranes are applied as separators,

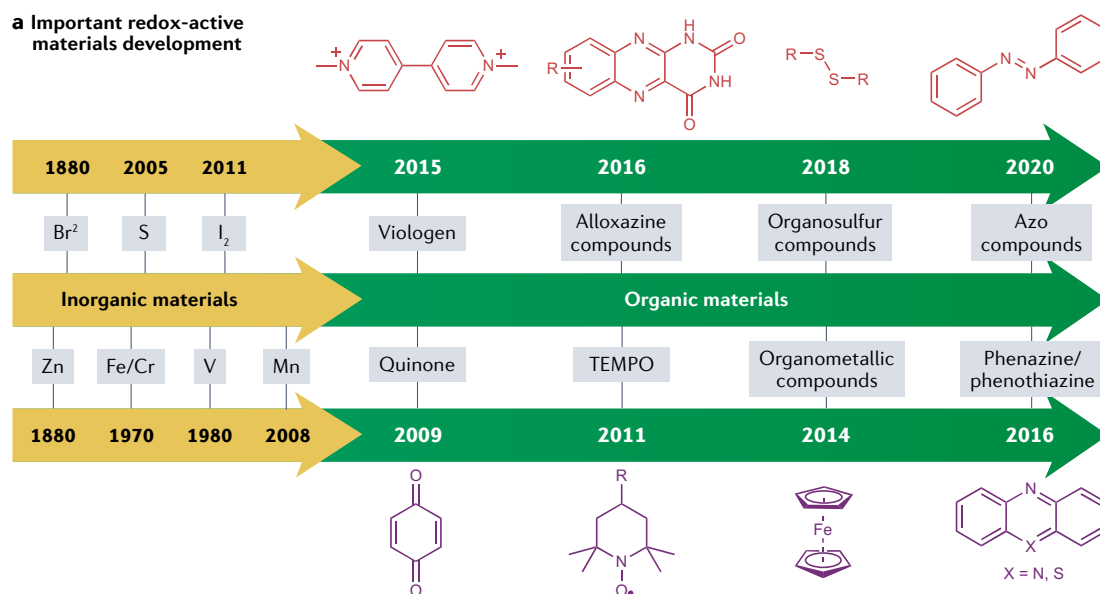
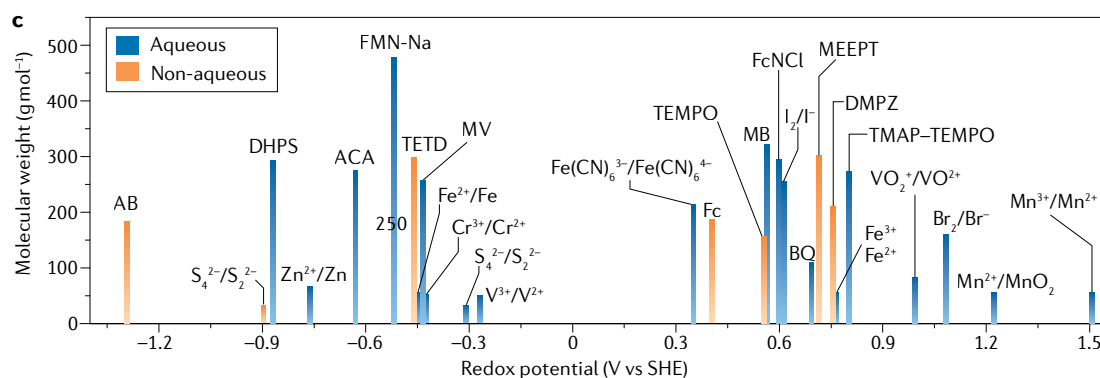
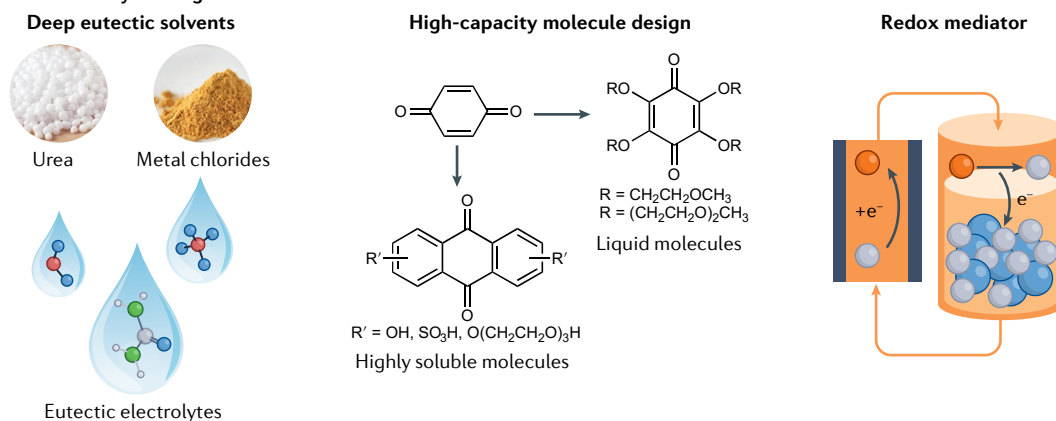
respectively. At the anode, the reaction is the reversible stripping/deposition of metals. **c** | Schematic of a semi-solid RFB with solid active materials and carbon black suspended in liquid electrolytes or energy storage tanks (redox-targeting design), respectively. **d** | A solar flow battery in which a photoelectrode is integrated into the system. During the charging process, the photoelectrode absorbs solar energy, which is used to reduce the redox species in anolyte. **e** | Reported working voltage ranges for various RFB types. **f** | Summarized efficiency of various RFB types (black, Coulombic efficiency; red, voltage efficiency; all other colours, energy efficiency).

anolyte and catholyte, respectively, are stored in separate external tanks and circulated by pumps to flow through porous carbon electrodes, driving the redox reactions. The anolyte and catholyte are separated by an ion-conductive membrane with high charge-carrier selectivity, thus balancing the charge transfer during charging and discharging. RFBs are usually categorized, by the solvents used in the electrolytes, into aqueous and non-aqueous systems. Solid-state separators have been used to enable the development of hybrid systems that employ a combination of aqueous and non-aqueous electrolytes<sup>12</sup>. Early studies focused on aqueous systems, using inorganic metal salts as soluble redox-active materials. In recent years, non-aqueous RFBs have attracted increasing attention because organic electrolytes can provide a wider potential window, which is beneficial for the development of high-voltage, high-energy systems<sup>13</sup>.

In a typical RFB, the important components are the electrolyte, electrode and membrane. Dissolving in the electrolyte, the soluble redox-active materials are the energy storage component that establishes limits for overall battery performance, including voltage, capacity and cycling stability. Most recently reported work to date has focused on the design of high-capacity and stable organic redox-active materials and understanding the effect of different functional groups on solubility, stability, reversibility and redox potential<sup>14</sup>. Additionally, it is also important to explore new molecular structures for reversible reactions and to advance our understanding of the underlying mechanisms of both electron transfer reactions and possible decay mechanisms. Membranes applied in RFBs can be divided into two main categories: dense (for example, Nafion) or porous (for example, Daramic)<sup>15,16</sup>. There is increasing interest in finding new cost-effective dense membranes consisting of rigid polymer backbones and functional side chains to decrease solvent swelling and maintain high conductivity<sup>17–22</sup>. As new redox chemistries move away from the highly acidic and oxidative metal ions, there may be a greater material and design space for new membranes<sup>23–26</sup>. The current lack of organic-solvent-compatible membranes is a critical challenge for the application of non-aqueous RFBs<sup>27,28</sup>. Yet, limited studies have been conducted in non-aqueous solvents to advance the fundamental understanding of rational design of membranes towards low crossover of redox-active materials. The performance of RFBs is often dominated by the electrodes. Porous carbon materials, such as graphite felt or carbon paper, are commonly employed as electrodes owing to their high electron conductivities and large surface areas. Given that the redox reactions occur at the electrode surface and must be accompanied by the circulation of electrolytes, the rational design of porous structure and flow channels is of high importance for performance analysis<sup>29–31</sup>.

With the continuous pursuit of better flow battery chemistries, new designs and material systems, beyond conventional RFBs, have emerged in recent decades<sup>32,33</sup>. The flow battery concept has the advantage of design flexibility, such that many other typical energy storage chemistries, such as metal deposition/dissolution (Li, Zn or Al)<sup>12</sup>, photoelectrochemical reaction<sup>34</sup> and solid

intercalation chemistry<sup>35</sup>, can be integrated into the flow system to create new types of flow batteries (hereafter referred to as next-generation flow batteries). To increase energy density, metal deposition chemistry, with low redox potentials and high capacity, can be adapted to combine with the flow battery (FIG. 1b); these technologies are called hybrid RFBs<sup>12</sup>. For example, Li-metal-based flow batteries can achieve a voltage of over 3 V, which is beneficial for high-energy systems. As the metal anode reaction is a stripping/deposition process, the independence of energy and power characteristic of RFBs does not apply fully to hybrid systems. However, they can still share some similar advantages to conventional RFBs, because the reaction occurring in the cathode side is the same as that in conventional RFBs, and many applied metals can work at relatively high current densities. For example, Zn-based flow batteries have the advantages of low cost, high capacity, high power and inherent stability in air and aqueous solutions<sup>36</sup>. Many Zn-based flow batteries have been demonstrated to operate stably at current densities greater than 80 mA cm<sup>-2</sup> and can also achieve power densities of more than 1,000 mW cm<sup>-2</sup> (REF.<sup>37</sup>). However, for practical applications, it is important to further consider Coulombic efficiency and dendrite issues. In FIG. 1c, the recently explored concept of a semi-solid flow battery is shown; in this technology, the flow features remain while enhancing energy density by suspending energy-dense solid active powders (that is, sulfur, LiCoO<sub>2</sub>, LiFePO<sub>4</sub>, etc.) and conductive additives into flowable liquid electrolytes. This approach overcomes the solubility limit<sup>38–40</sup>; however, the high viscosity of slurry-like electrolytes can create complex fluid dynamics and result in limited reaction kinetics, thus compromising the efficiencies and increasing maintenance costs. Another approach that combines liquid and solid redox chemistry for semi-solid energy storage is redox-targeting flow batteries that use soluble redox species as mediators to achieve redox-targeting reactions of solid battery materials to improve the energy output<sup>41–43</sup>. To successfully extract the charge from solid materials via the redox-mediated reaction, the potential of active species should match the Fermi level of the applied battery material<sup>44</sup>. More recently, by combining solar photovoltaic technologies and rechargeable batteries, it has become possible to integrate solar energy conversion and electrochemical energy storage. Taking advantage of flexible flow battery design, the semiconductor photoelectrode can be monolithically integrated into the flow battery. This technology, which is called a solar RFB, presents a new approach for designing highly efficient solar energy utilization systems and has received increasing research interest<sup>45,46</sup> (FIG. 1d). The general working principle of solar RFBs is that solar energy is absorbed by the photoelectrode to generate photoexcited carriers to drive the oxidation or reduction of redox species. In comparison with separate devices, solar RFBs could offer some advantages, such as (1) cost reduction for the electrical management systems, (2) heat removal by the flowing electrolytes and (3) higher photoconversion efficiency (solar energy input to electrical energy output) and solar power conversion utilization ratio as a result of better voltage matching and reduced energy conversion

**a Important redox-active materials development**

**b New electrolyte design**


losses. However, the development of long-lived solar RFBs remains a challenge because of corrosion that occurs at the photoelectrodes upon contact with active electrolytes. In FIG. 1e,f, we present the working voltage and efficiency information of various RFB types.

Designing promising redox-active materials in terms of both energy density and stability is the major scientific challenge for flow batteries, and is also the most important foundation for further advancement of next-generation RFBs. For example, the rational design of both redox-targeting and solar flow batteries is highly dependent on a greater choice of suitable redox species

that enable a good match in different aspects, including voltage, chemical compatibility and electrochemical stability. Organic molecules have been recently proposed and widely studied as promising alternatives for RFBs, and it has become the major research trend in this discipline<sup>14,47,48</sup>. Notably, taking advantage of flowable redox-active materials and flexible structure designs, the flow systems can be further extended to approach the challenges of water desalination<sup>49</sup> or to assist with the development of synthetic chemistry, such as in the direct electrosynthesis of aqueous H<sub>2</sub>O<sub>2</sub> (REFS<sup>50,51</sup>), CO<sub>2</sub> reduction<sup>52</sup> and cross-coupling reactions<sup>53–56</sup>.

◀ Fig. 2 | **Development of representative materials chemistry for redox flow batteries.**

**a** | Timeline of important inorganic and organic redox-active materials in the development of redox flow batteries. Red molecules are used as anolytes, generally, and purple molecules are used as catholytes (also note that phenazine can be used as anolyte in aqueous systems). **b** | Recent advances in highly concentrated electrolyte designs enable high-capacity redox flow batteries. **c** | Redox potential of various redox-active materials. AB, azobenzene; ACA, alloxazine 7/8-carboxylic acid; BQ, benzoquinone; DHPS, 7,8-dihydroxyphenazine-2-sulfonic acid; DMPZ, 5,10-dihydro-5,10-dimethyl phenazine; Fc, ferrocene; FcNCl, (ferrocenylmethyl)trimethylammonium chloride; FMN-Na, riboflavin-5'-monophosphate sodium; MB, methylene blue; MEEPT, N-(2-(2-methoxyethoxy)-ethyl) phenothiazine; MV, methyl viologen; SHE, standard hydrogen electrode; TEMPO, 2,2,6,6-tetramethylpiperidine-1-oxyl; TETD, tetraethylthiuram disulfide; TMAP-TEMPO, 4-[3-(trimethylammonio)propoxy]-2,2,6,6-tetramethylpiperidine-1-oxyl chloride.

### New chemistry and materials design

From the zinc-bromide battery to the alkaline quinone flow battery, the evolution of RFBs mirrors the advancement of redox chemistry itself, from metal-centred reactions to organic molecular designs<sup>57</sup>. A range of novel redox species and design concepts have been proposed and developed for next-generation flow batteries in recent years. The chemistries of redox-active materials in aqueous and non-aqueous systems are reviewed below, including their specific characteristics and intrinsic limitations. We focus our overview on the representative progress in inorganic-based and organic-based redox-active materials, highlighting recent advances in organic redox molecules for RFB applications.

**Aqueous redox chemistries.** The redox chemistries applied in aqueous and non-aqueous systems have unique characteristics. Water is a polar solvent with a high dielectric constant, so most supporting salts exhibit high solubilities with sufficiently dissociated ions, leading to high conductivity ( $>100 \text{ mS cm}^{-1}$ )<sup>58</sup>. Consistently, the ion-exchange membrane (that is, Nafion) with water swelling can enable an impressive ion conductivity ( $50\text{--}200 \text{ mS cm}^{-1}$ )<sup>59</sup>. As a result, advanced aqueous redox chemistries<sup>60</sup> can achieve a power density that is higher than  $500 \text{ mW cm}^{-2}$ . However, the main disadvantage of water is its limited potential window ( $<2 \text{ V}$ )<sup>61</sup>, which prevents the use of materials whose redox potentials lie outside this range. Up to now, redox chemistries in aqueous electrolytes have been the most appealing options for RFBs because they not only enable high concentration but also offer the merits of good safety, fast kinetics and economic sustainability<sup>62</sup>. At the time of writing, state-of-the-art redox chemistries in aqueous systems have high diffusion coefficients (such as  $>10^{-6} \text{ cm}^2 \text{ s}^{-1}$ ) and kinetic rate constants (such as  $>10^{-1} \text{ cm s}^{-1}$ ), and can also achieve high capacities (such as  $>53.6 \text{ Ah l}^{-1}$ ) and long-term stability ( $<0.01\%$  capacity loss per cycle,  $0.01\text{--}0.1\%$  per day). Given the water solvation, the effect of protonation as well as hydroxide addition on the redox reactions that accompany intermolecular electron transfer must be taken into consideration. In addition, the detailed mechanism of electron transfer dynamics involved in the one-step/two-step one-electron or one-step two-electron reactions needs to be studied further to achieve a comprehensive understanding. Additionally, aqueous redox chemistries can be greatly affected by large fluctuations in ambient temperature because water exhibits a narrow operational temperature range ( $0\text{--}100^\circ\text{C}$ )<sup>63</sup>.

**Non-aqueous redox chemistries.** Although many alternative solvents are available for non-aqueous reactions, redox-active materials often show only limited solubility ( $\sim 0.1 \text{ M}$ )<sup>64,65</sup>. Meanwhile, although diffusion coefficients are similar ( $10^{-5}\text{--}10^{-6} \text{ cm}^2 \text{ s}^{-1}$ ), sluggish reaction kinetics are often observed in non-aqueous electrolytes, together with low conductivity (approximately  $<50 \text{ mS cm}^{-1}$ ), all of which results in inferior power density (typically  $<100 \text{ mW cm}^{-2}$ ). Organic solvents also face more stringent safety issues and are more expensive. However, rational screening of organic solvents is able to provide wide operational temperature ranges and potential windows, which enable the design of high-voltage RFBs that can operate in extreme environments and the feasible use of alkali-metal anodes<sup>66</sup>. The relative permittivity is an important parameter that should be considered for organic solvents, given the influence on solubility and supporting salt dissociation<sup>13</sup>. For now, because of their relatively high conductivities and facile dissolution of promising organic redox-active materials, acetonitrile, 1,2-dimethoxyethane, and *N,N*-dimethylformamide are widely used as solvents. As chemical decomposition is a typical problem in non-aqueous systems, systematic analysis of factors influencing the stability of organic radicals must be performed<sup>67</sup>. The fundamental understanding of redox chemistry in non-aqueous systems is also less well studied<sup>68</sup>. For example, some redox-active molecules exhibit one-step two-electron transfer reversible reactions in aqueous electrolytes, while in a non-aqueous electrolyte, the same molecules undergo two-step one-electron transfer; this needs to be further understood both deeply and systematically. The state of development of non-aqueous redox chemistries lags behind that of aqueous systems in terms of available redox-active materials, appropriate selectively ion-conductive membranes and demonstrated performance. In non-aqueous systems, the choices of highly soluble (that is,  $>1 \text{ M}$ ) and chemically stable redox-active materials are limited, and the lack of high-performance membranes make the performance analysis of non-aqueous systems very difficult because of serious crossover issues, which can also cause problems in performance comparison.

**Development of redox-active materials.** The key redox-active materials of RFBs and their development are summarized in FIG. 2. Solubility is of particular importance, and we propose the rubric in BOX 1 to both classify and discuss the solubility of different redox-active materials employed in RFBs under different conditions.

A timeline for the development of representative redox species for RFB applications is shown in FIG. 2a. For much of the past century, chemistries for RFBs were focused mainly on inorganic redox species, such as bromine, iodine, sulfur, vanadium, iron or manganese<sup>32</sup>. These inorganic materials generally offer good chemical stability with the capability of rebalancing after crossover, fast reaction kinetics in aqueous solutions and few concerns about solubility. However, for each inorganic species, there are many specific problems. For example, the reversible redox chemistries of bromine and iodine species are highly sensitive to pH fluctuation<sup>69,70</sup>.

#### Rebalancing

Similar to regeneration, the recovery of active species following membrane crossover.



**Electrode passivation**

A decrease in active electrode surface area and an increase in contact and charge transfer resistance. Passivation is generally caused by the deposition and accumulation of side products on the surface of the electrode.

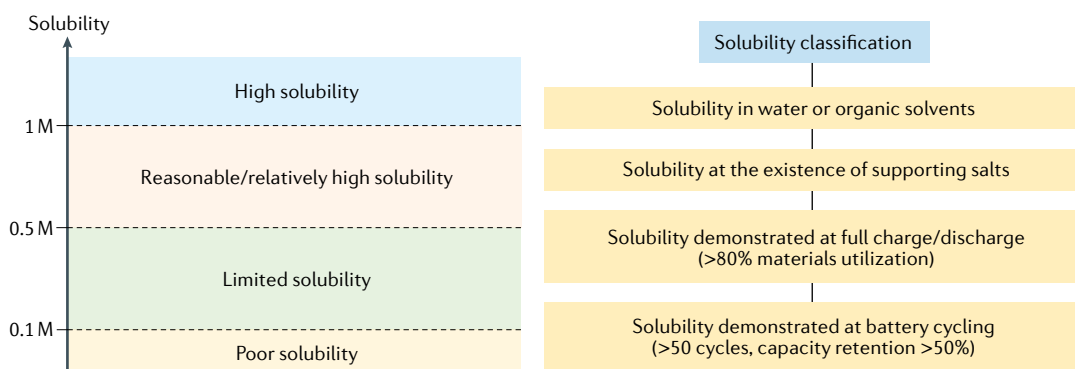
Vanadium species are expensive and require the use of strongly acidic electrolyte (3–4 M  $\text{H}_2\text{SO}_4$ )<sup>58</sup>. For sulfur, iron, chromium or manganese species, the occurrence of precipitation, hydrolysis or incomplete dissolution of the solid phase involved in battery operation significantly limits performance efficiency, and there is also an issue with electrode passivation<sup>71–73</sup>. In addition, most inorganic species suffer from the considerable crossover issues.

In recent years, organic or organometallic materials have attracted extensive interest as inexpensive and green alternatives for the design of advanced flow batteries. Such materials offer structural diversity, enabling tuning of their physical and chemical properties, high element abundance and minimal environmental concerns<sup>14,74</sup>. Early pioneering work focused on molecules with redox centres of C or O, such as quinones<sup>75–77</sup>, 2,2,6,6-tetramethylpiperidine-1-oxyl (TEMPO)<sup>78–80</sup> or methyl viologen (MV)<sup>79,81–83</sup>. More recently, attention has turned to designing molecules with redox centres at N or S, such as phenazine/phenothiazine<sup>84–89</sup>, organo-sulfur<sup>90,91</sup> and azo compounds<sup>92,93</sup>. Quinones are the most extensively studied organic molecules for RFBs, especially for aqueous systems. Redox reactions of the carbonyl group offer fast reaction kinetics, while the aromaticity stabilizes the reduced product<sup>94,95</sup>. In protic electrolytes, benzoquinone reduction to hydroquinone proceeds through a one-step two-electron transfer reaction<sup>75</sup>, while in aprotic electrolytes, two successive one-electron transfers are observed<sup>96</sup>. To improve the solubility (>1 M) and stability (fade rate <0.1% per day), a variety of anthraquinone structures have been designed and studied<sup>97</sup>. In contrast with quinones, the ketone in fluorenone derivatives can easily undergo two electron reductions in water to form hydroxyls and this is accompanied by irreversible formation of a benzylic C–H bond. This irreversible C–H bond formation leads to failure of fluorenone-based flow batteries. By incorporating electron-withdrawing groups and lowering the  $\text{pK}_a$  of the benzylic C–H, the reverse reaction can be achieved in aqueous alkaline media, leading to the reversible discharge of the material in battery content<sup>98</sup>. TEMPO is a representative nitroxide radical redox species, showing

stable redox chemistry (many cycles of oxidation and reduction can be conducted without obvious structural breakdown) in both aqueous and non-aqueous systems, with advantageous solubility, redox potential and kinetics<sup>99</sup>. Modification, by the addition of hydroxyl groups at the 4-position, increases the solubility from near zero to 2 M in water<sup>79</sup>. Some nitroxide radicals were also found to undergo reversible reduction, showing their potential as new material candidates for RFBs<sup>100,101</sup>. Viologens are another widely explored organic molecule for aqueous RFBs; in those compounds, the heterocyclic aromatic rings act as the redox centre. MV<sup>2+</sup> (methyl viologen dication) is highly soluble in water, but the reduced product, charge-neutral MV, is barely soluble, and, moreover, dimer formation may also occur during the reduction process<sup>82</sup>. Therefore, previous work focused mainly on improving the solubility of the reduced product through functionalization with hydrophilic groups<sup>102</sup>. In recent work, nitrogen-containing heteroaromatic molecules are also used as promising redox-active materials for aqueous RFBs. For example, alloxazine compounds with the inclusion of amides/imides and carbonyls can provide a highly stable structure for electron transfer reactions because of the conjugated structure with high resonance<sup>103</sup>. In addition, the carboxyl group confers a significant improvement solubility of up to 2 M in alkaline electrolytes<sup>104</sup>. By substituting nitrogen or sulfur for the carbon in the central ring of anthracene, the cooperation of aromaticity and a large resonance stabilization effect between carbon and the heteroatoms enhances stability of the reduced product. 7,8-Dihydroxyphenazine-2-sulfonic acid (DHPS) is highly soluble (up to 1.8 M) in 1 M KOH, which has been attributed to the location-specific intensified solvation (the asymmetric charge distribution in phenazine core enhances the dynamic interaction with the solvent)<sup>86</sup>. For phenothiazine derivatives, methylene blue (MB) also achieves high solubility (1.8 M) via rational electrolyte optimization, with stable cycling achieved even at high concentrations (>1 M)<sup>87</sup>. Metal–ligand complexes, especially iron-based species<sup>14</sup>, have also been explored in aqueous systems, and, recently, iron complexes with

**Box 1 | Solubility standard and classification**

We propose the solubility standard to evaluate the solubility level of redox-active materials. In addition, it could also be important to revisit solubility under different conditions, such as the existence of supporting salts, change of oxidation/reduced states and demonstrated solubility during cycling. Future research should consider the solubility classification for further clarification.



## Hydrotropic effect

The use of suitable organic additives (for example, urea) to help increase the solubility of redox-active solute in aqueous solution through intermolecular interactions (for example, hydrogen bonding).

2,2'-bipyridine-4,4'-dicarboxylic acid and cyanide ligands were reported to exhibit a high solubility of 1.2 M with considerable stability (fade rate, 0.25% per day) due to a symmetry-breaking design<sup>105</sup>.

Metal–ligand complexes have previously been applied as the redox-active components of non-aqueous RFBs, but, generally, their limited solubility (<0.5 M) in these solvents is a big barrier for performance metrics. Ferrocene has both reasonable solubility (>0.5 M) and suitable redox potential to qualify<sup>106</sup>. Additionally, the incorporation of ionic functional groups such as quaternary ammonium or anionic sulfonate groups into ferrocene can significantly enhance solubility and improve viability<sup>107,108</sup>. Although the properties of metal–ligand species also can be tuned through the selection of organic ligands, advanced metal–ligand complexes with high solubility, redox potential and stability are reported only infrequently. In recent years, more efforts have been made to design soluble metal–ligand complexes (with solubilities >0.1 M) for non-aqueous systems. Some advanced candidates have been demonstrated to have solubilities in excess of 0.5 M (REFS<sup>109–111</sup>). The adoption of organic molecules in non-aqueous systems has been explored far less, and many reported organics show limited solubility and suffer from poor stability. Recently, phenazine derivatives with added 2-methoxyethyl chains at nitrogen positions can obtain an enhanced solubility (0.5 M) in organic solvents<sup>88</sup>. Azobenzenes are a relatively new group of redox-active species that can be applied in RFBs. The hydrophobic scaffold means that these molecules are highly soluble (>1 M) in many common organic solvents<sup>92</sup>. The  $\pi$ -conjugated molecular structure promotes good chemical and electrochemical stability, enabling long-term stable cycling in non-aqueous electrolytes. In addition, by rational modification with hydrophilic groups, the azobenzene-based derivatives can also be used as redox-active materials for aqueous RFBs<sup>93</sup>. Organosulfides are also potential alternatives for non-aqueous RFBs due to abundant sulfur resource and high solubility. However, sluggish kinetics, poor reversibility and insoluble phase precipitation impede the use of sulfur-based redox chemistry in RFBs. The strategy of asymmetric allyl-activation has been used to improve its reaction kinetics and reversibility<sup>90</sup>. Meanwhile, it was found that the tetraethylthiuram disulfide molecule has the following promising features for non-aqueous systems: ultralow material cost, stable resonance structure, high solubility and reversible redox chemistry without insoluble phase formation<sup>91</sup>. In addition to these, some other highly soluble organic molecules (>1 M) were also identified, such as quinoxaline<sup>112</sup>, 9-fluorenone<sup>67</sup>, 2,1,3-benzothiadiazole<sup>113</sup>, 2,5-di-tert-butyl-1-methoxy-4-[2'-methoxyethoxy]benzene (DBMMB)<sup>114</sup>, phenothiazine<sup>84</sup>, polycyclic aromatic hydrocarbons<sup>115</sup>, N-methylphthalimide<sup>116</sup> and TEMPO<sup>78</sup>.

**High-capacity electrolyte design.** To develop high-energy RFBs — to improve capacity without simply increasing the working voltage — several new electrolyte designs have been proposed, including the use of deep eutectic solvents<sup>117,118</sup>, liquid molecules<sup>114</sup>, redox mediator strategy<sup>35</sup> or multi-redox species<sup>119</sup>.

A typical deep eutectic solvent is composed of large, asymmetric ions with delocalized charges, which leads to a reduced lattice energy and lowered freezing points. They are usually prepared through the complexation of a quaternary ammonium salt with a metal salt or a hydrogen bond donor<sup>118</sup>. For instance, specific ratios of  $\text{FeCl}_3 \cdot 6\text{H}_2\text{O}$  and urea are known to form a brown liquid at room temperature<sup>120</sup>. Most deep eutectic solvents used in flow batteries are metal-based with a high concentration of active species (3–6 M)<sup>121</sup>, in which the metal centre is the redox-active component. The working principle is dependent on the valence state and coordination change of the metal centres. Organic-based eutectic electrolytes can also be produced by involving appropriate organic redox-active materials with inorganic/organic compounds (such as mixing *N*-methylphthalimide, lithium bis(trifluoromethanesulfonyl)imide and urea)<sup>122</sup>. Another approach to high capacity is the design of highly soluble or even the use of liquid molecules. For high solubility, a general rule is 'like dissolves like.' Therefore, molecules with highly hydrophilic structures can better dissolve in water, while hydrophobic molecular scaffolds tend to dissolve in organic solvents. To increase water solubility, hydrophilic functional groups can be applied to strengthen the solvation effect. Thus, hydroxy, sulfonic, carboxylic and amino groups are frequently used in the molecular functionalization because of their high polarity and hydrophilicity<sup>14</sup>. For example, by functionalizing with hydroxy and sulfonic groups, the solubility of phenazine derivatives in aqueous systems can be increased from near zero to 1.8 M (REF.<sup>86</sup>). Likewise, non-polar groups can be used to enhance the solubility in non-aqueous solvents. It is important to have the localized asymmetry in the molecular structure to obtain a high solubility<sup>86</sup>. Adding functional additives may also help to enhance the solubility. For example, urea can significantly increase the water solubility of hydroquinone by the hydrotropic effect<sup>123</sup>. For liquid molecule design, it is known empirically that the addition of methyl and methoxy groups or poly(ethylene oxide) chains can help to produce compounds with low melting points, such as 1,1'-dimethylferrocene<sup>124</sup> or DBMMB<sup>114</sup>. Similarly, ethylene glycol mono methyl ether or diethylene glycol mono methyl ether groups have been reported to lower the melting point of quinone molecules<sup>125</sup>. Although the use of liquid molecules has the potential to maximize capacity, their high viscosity and problematic dissociation of supporting salts can make them challenging for use in RFBs.

In a redox-targeting design, solid particles of active materials are stored in the external tanks and do not flow through/past the electrode. Instead, redox mediators are applied to complete the electron transfer process. By combining the solid and liquid redox chemistries, the redox-targeting electrolyte can deliver a much higher capacity<sup>43</sup>. To achieve electron transfer between redox mediators and solid active materials, the redox potential of solid active materials should be in the middle of that of the redox mediators<sup>35</sup> (FIG. 2b). Given that the overall reaction process involves multiple electron transfers, the current capability of this RFB chemistry remains limited.

**Capacity utilization**  
The percentage of delivered capacity over theoretical capacity.

Theoretically, the design flexibility of organic materials can enable the creation of multi-redox species capable of large numbers of electron transfers (BOX 2); however, in practice, most reported organic materials only exhibit one or two reversible electron transfers. The problem arises because the addition of a redox-active moiety to the molecular structure may result in significant changes to the solubility, chemical stability and reaction reversibility of active centres already present. For example, the polymerization of redox-active molecules is able to easily increase electron transfer numbers, but it can lead to a significant decrease in the solubility and affect the reaction kinetics. A few polyoxometalates<sup>126</sup> or metal–ligand complexes<sup>127</sup> have intrinsically high electron transfer numbers and can also show a reasonable solubility (that is, >0.5 M). However, their multi-redox reactions usually show multiple pairs of peaks of reversible reactions in the cyclic voltammetry (CV) curves, which can lead to difficulty in finding a potential match of catholytes and anolytes or capacity utilization in the RFB demonstration.

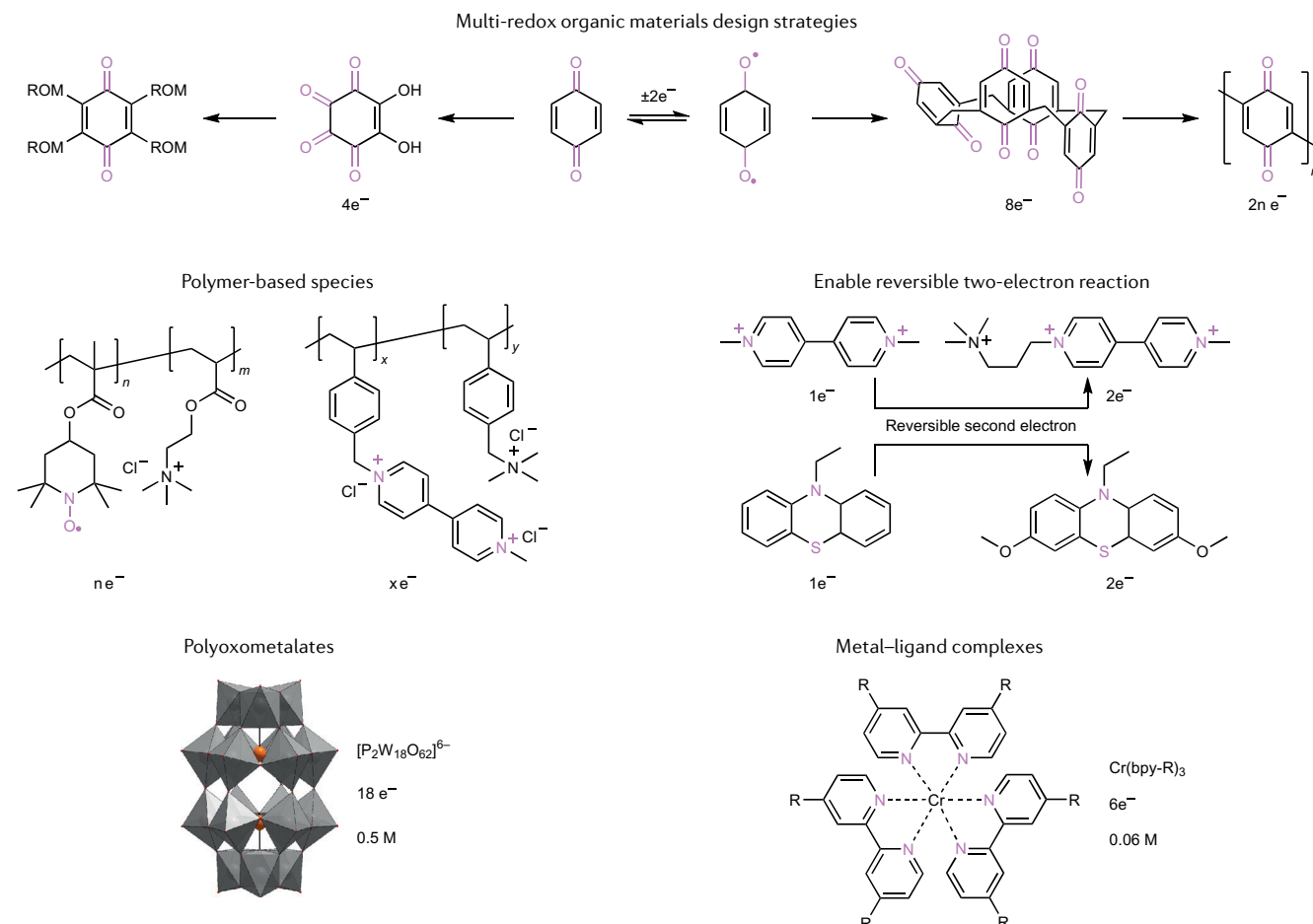
**General design philosophy.** In this subsection, we further summarize the general design philosophy for redox-active materials. From a practical point of view, the materials design should include: (1) reversible redox activity, (2) high solubility, (3) scalable synthesis with low cost, (4) fast kinetics, (5) long lifetime, (6) appropriate redox potential and (7) environmental sustainability and resource recycling. Particularly, to design highly soluble organic molecules, the dielectric constant should first be considered. For aqueous systems, hydrophilic molecular structures and functional groups are preferred. High polarity and local structure asymmetry of substituted functional groups may also be beneficial to improving solubility. A similar principle applies to non-aqueous systems. For electrochemical activity, the redox centres (for example, C, N, O, S) must be properly distributed in the molecular structure to either avoid the formation of possible radicals or stabilize the radical. Another important consideration for redox-active materials design, especially for organic systems, is the

## Box 2 | Strategies for increasing the electron transfer numbers of redox-active materials

Organic redox-active materials have attracted growing interest because of their structure diversity with the capacity for tuning solubility, stability, redox potentials and even electron transfer numbers. To increase the capacity, in addition to improving solubility, increasing electron transfer numbers is also an effective method. Thus, we summarize some possible strategies to increase electron

transfer numbers and some redox-active materials that can undergo multielectron transfer reactions (for example,  $\geq 2$ ), including organic molecules/polymers, polyoxometalates and metal–ligand complexes.

Note that the listed solubility is the one demonstrated in the electrochemical test. ROM, redox-active organic molecule.



The polyoxometalate structure is adapted with permission from REF.<sup>119</sup>, Springer Nature Ltd.



## Crossover effect

An effect, including, for example, capacity decay and side reactions, that occurs as a result of penetration of the redox species through the membrane.

long-term stability under operating conditions. Whether an aqueous or a non-aqueous electrolyte is used, the formation of a conjugated or aromatic structure may help to enhance the stability. Designing a resonance structure, adding electron-donating groups in the forming organic radicals or introducing functional groups with high steric hindrance may provide the stabilization effect in non-aqueous systems. In addition, to mitigate the crossover effect on the apparent stability, researchers also developed the size-exclusion concept by synthesizing the oligomer,<sup>128–130</sup> polymer,<sup>131–133</sup> or bipolar molecules<sup>134</sup>.

FIGURE 2c presents the redox potential of various redox-active materials. This is an intrinsic property of redox-active materials that, in the case of metal ions, can be affected by ligand coordination or, in the case of organic molecules (such as quinones), the pH environment. For example, an Fe<sup>II</sup> redox centre shows an anodic shift of 700 mV in CV curves when the coordination ligand is changed from CN<sup>−</sup> to Dcbpy<sup>2−</sup> (REF.<sup>105</sup>). Similarly, high pH is reported to be preferable when riboflavin-5'-monophosphate sodium species is the anolyte, as it results in improved redox activity and a cathodic shift of redox potential<sup>103</sup>. Importantly, electron-donating groups can be introduced to decrease redox potentials of negative species and, likewise, electron-withdrawing groups can be used to increase the redox potentials of positive species. Moreover, it was reported the hydroxyl group as electron-donating group can provide a large cathodic shift (>400 mV) in redox potential for phenazine<sup>86</sup> or alloxazine<sup>104</sup> molecules.

The reaction kinetics are rather more an inherent property of the redox-active materials, although the supporting electrolyte can play a role. In order to further improve reaction kinetics, it is important to understand the detailed reaction mechanism. It is also worth noting that most reported organic redox-active materials can achieve a diffusion coefficient of 10<sup>−5</sup>–10<sup>−6</sup> cm<sup>2</sup> s<sup>−1</sup> and a kinetic rate constant of 10<sup>−2</sup>–10<sup>−3</sup> cm s<sup>−1</sup>. These figures are generally comparable with or superior to that of vanadium species. For organic redox-active materials in particular, it is critical to factor in the cost of convenient and scalable synthesis in assessing the economic viability of all-organic-based RFBs. Future studies may also be required to explore the relationship of the purity of redox-active materials and their performance. Cost analysis has shown that, for practical implementation, a target price of \$5 kg<sup>−1</sup> is feasible for redox-active organic materials<sup>135</sup>. It is still necessary to consider the recycling of resources as well as methods to regenerate redox-active materials.

## Performance assessment and decay mechanisms

Understanding the dominant decay mechanisms of flow battery performance helps to guide the rational design of promising redox-active materials, as well as appropriate assessment methods that can directly probe the limiting processes. The major degradation mechanisms can be categorized into intrinsic chemical and electrochemical stability of redox-active materials, membrane crossover issues and electrode passivation. In addition, it is also important to discuss how each of these decay mechanisms affect the relative importance

of time-dependent or cycle-denominated performance metrics (for example, timescale, cycle numbers, current density, concentration, etc.)<sup>136</sup>. Building critical testing methods for different RFBs is beneficial for performance comparisons.

**Electrochemical performance analysis.** When investigating new redox-active materials for RFBs, an essential first step is to evaluate the intrinsic physicochemical properties of the redox species, including its solubility, chemical stability, redox potential, along with the reversibility and kinetics of the proposed redox reaction. The final three items in this list can be evaluated using CV and rotating disk electrode (RDE) studies<sup>137,138</sup>. The redox reaction can be classified into three types: reversible, irreversible and quasi-reversible reactions. Typical CV curves for reversible or quasi-reversible reactions at different sweep rates are shown in FIG. 3a, which can be indicated by the potential difference ( $\Delta E_p$ ) or ratio of currents ( $i_{pa}/i_{pc}$ ) of oxidation and reduction peaks. The experimental conditions, such as the reference electrode, the concentration of supporting salts and redox species, and sweep rate, can all influence the CV results. Furthermore, electrochemical stability is indicated by constant peak intensity position and shape within the cyclic voltammogram.

The kinetics of the redox reaction — including the diffusion coefficient and the reaction rate constant — are important factors in the current capability and energy efficiency of RFBs, and can also be studied using CV. The diffusion coefficient can be calculated based on the Randles–Sevcik equation. To probe reaction kinetics in CV curves, Nicholson's method is commonly applied to estimate rate constants with application limits, and a representative example using this method can be found in the work of Luo et al.<sup>139</sup>. It should be noted that the equations applied to calculate reaction kinetics may differ with the reaction type<sup>138</sup>, and this should be carefully considered and qualified in order that the results are consistent and comparable.

In RDE studies, the diffusion current is related only to the diffusion and the rotation rate (and is independent of the electrode potential or the reaction rate). These studies can, thus, be applied to all reaction systems, including irreversible and quasi-reversible systems. At a specific rotation rate, the steady flux of anolyte or catholyte to the electrode surface leads to a constant current (FIG. 3b). Based on the linear sweep voltammetry curves at different rotation rates, the diffusion coefficient can be determined using the Levich equation. RDE studies can also be used to check the rate constant of redox species using the Koutecký–Levich and Butler–Volmer equations (FIG. 3c). A detailed example for the RDE study of anolyte and catholyte can be found in the work of Wei et al.<sup>116</sup>. RDE studies are preferable to CV characterization for accurate determination of redox reaction kinetics<sup>138</sup>.

With a large number of new chemistries being reported as being useful for RFBs, the development of performance assessment methods and standardized testing frameworks is important<sup>140</sup>. Only with such methods in place is it possible to avoid the inconsistency and ambiguity of performance comparisons. Performance

**Capacity fade rate**

The loss in capacity, usually expressed as a percentage, over the total cycle number (% per cycle) or test time (% per day).

reporting for aqueous systems is more mature and consistent compared with non-aqueous systems, because, as it stands, there is no appropriate membrane for organic electrolytes. Generally, the asymmetric full-cell demonstration is the most important for performance assessment of all RFB chemistries.

The two most important performance metrics are the working voltage and capacity (FIG. 3d). Working voltage directly affects the power and energy densities of RFBs<sup>141</sup>. The theoretical capacity value is dependent only on the concentration of redox species, but the actual capacity is not only dependent on the intrinsic properties (kinetics) but can also be influenced by device engineering (that is, cell resistance and flow conditions). Thus, at different current densities, the deliverable capacities and overpotentials are the indicators that reflect the current capabilities of RFBs. In addition, capacity utilization is also a common parameter reported in the literature. Plots of voltage and power density against current density give a polarization curve (voltage,  $E$  versus current,  $I$ ) which is used to determine the maximum power density (FIG. 3e), which is controlled by the voltage losses with current densities. The major factors for voltage loss are: (1) slow reaction kinetics — if the reaction is slow, then voltage will drop rapidly when current density increases, (2) cell resistance associated with electric contact and ionic conductivities of membrane and electrolytes and (3) mass transfer dynamics inside porous carbon electrodes. More importantly, capacity fade evaluation together with the efficiency data during the long-term cycling (FIG. 3f) are critical metrics for accessing the potential of RFBs for large-scale energy storage. Practically speaking, long-term stability at a reasonable energy density can

reduce maintenance and capital costs<sup>142</sup>, approaching low total active costs for long-duration energy storage. The capacity fade rate should be reported on deeply accessed capacity (performance data from shallow cycling are not reliable for evaluating long-term stability) and both the fade rates based on cycles and time need to be presented. Some recently reported organic redox-active materials have capacity fade rates as low as less than 0.02% per day, demonstrating that organic molecules can meet the lifetime requirements for practical use<sup>136</sup>. It is recommended that sufficient information be listed regarding experimental conditions as the reference for performance demonstration. In addition to capacity loss, the energy loss during long cycling is directly related to the energy efficiency, reflecting the variation of internal resistance for highly reversible systems. Most reported RFBs to date focus on demonstrating the following metrics: volumetric capacity and energy density, capacity fade rate and efficiencies, with the determination of reaction kinetics. In aqueous systems, MB and 1-methyl-1'-[3-(trimethylammonio)propyl]-4,4'-bipyridinium trichloride<sup>82</sup> were reported to show a higher kinetic rate constant of over  $0.3 \text{ cm s}^{-1}$ , while most other redox species have a value of  $10^{-2}$ – $10^{-3} \text{ cm s}^{-1}$ . When compared with other RFB systems, MB, DHPS, polysulfide, iodide or quinone-derivative-based systems are able to achieve a higher capacity of  $70 \text{ Ah l}^{-1}$  (based on single electrolyte). Meanwhile, the DHPS/ $\text{Fe}(\text{CN})_6^{3/4-}$  system can realize the higher energy density of  $\sim 100 \text{ Wh l}^{-1}$ . If hybrid systems are included in the comparison, Zn-based or Li-based systems may have the highest energy density ( $>150 \text{ Wh l}^{-1}$ ). In addition, the lowest capacity fade rate ( $<0.001\%$  per cycle,  $<0.01\%$  per day) has been

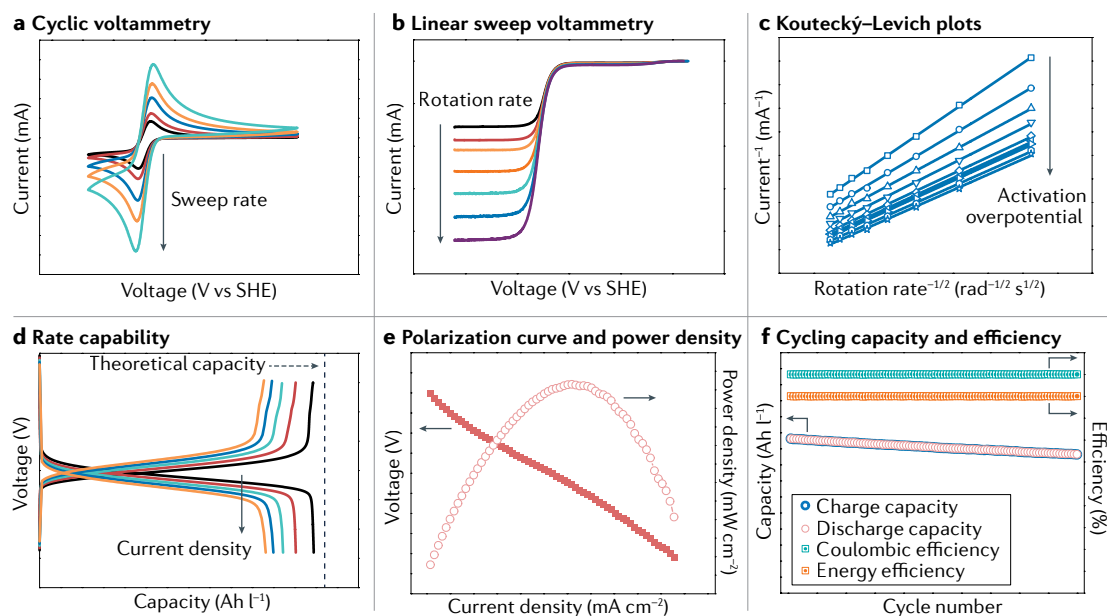


**Fig. 3 | Evaluation of electrochemical properties and performance assessment.** **a** | Cyclic voltammetry curves of redox-active materials at different sweep rates for electrochemical analysis (redox potential, reversibility, diffusion coefficient and electron transfer rate constant). **b** | Linear sweep voltammetry scans to study reaction kinetics. **c** | Koutecký–Levich plots for the calculation of electron transfer rate constant. **d** | Galvanostatic test of the flow battery with specific concentrations of electrolytes at different current densities for evaluating the capacity utilization and current capability. **e** | Polarization curves of the flow battery for power density measurements. Power is the product of voltage and current. **f** | Cycling measurement in terms of capacity and efficiency data. SHE, standard hydrogen electrode.

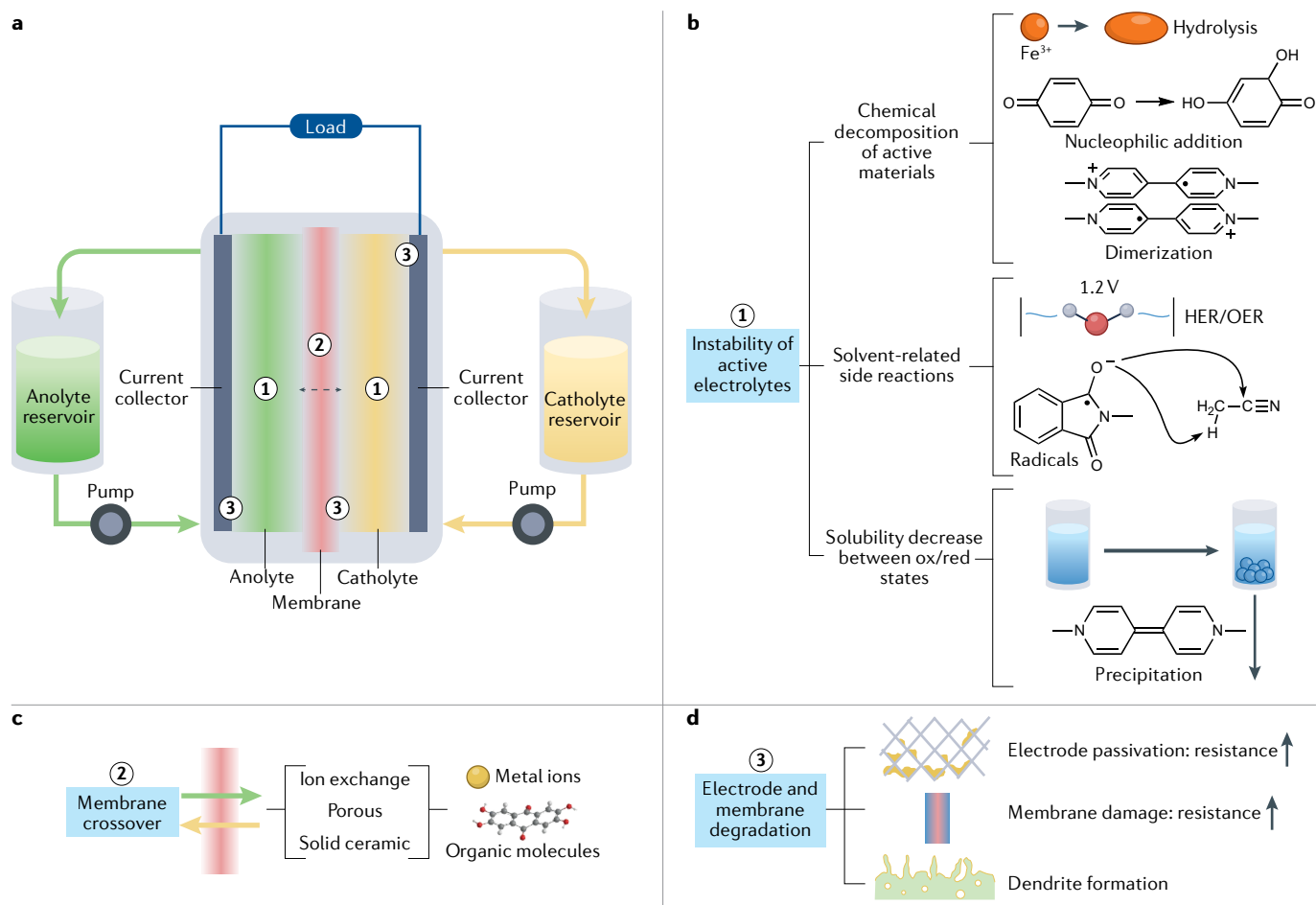


**Fig. 4 | Capacity loss mechanisms in redox flow batteries.** **a** | Schematic representation of possible capacity degradation in a redox flow battery. **b** | Schematic illustration of potential capacity fade mechanisms in electrolytes, including chemical decomposition, side reactions and solubility changes. **c** | Membrane-crossover-related capacity degradation. **d** | Capacity loss induced by electrode passivation (including dendrite formation in metal anodes) or membrane degradation. HER, hydrogen evolution reaction; OER, oxygen evolution reaction; ox, oxidized; red, reduced.

demonstrated for the quinone derivatives by applying a potentiostatic hold in the galvanostatic test<sup>143</sup>.

**Capacity loss mechanism and investigation.** We summarize here several key capacity-loss mechanisms for most RFB chemistries, including chemistry-dependent decomposition or component-related effects, and further discuss how it influences the flow battery testing method associated with capacity fade interpretation. The major mechanisms that cause capacity fade are: (1) instability of catholyte/anolyte, including chemical decomposition of redox-active materials, (2) crossover issues and (3) component degradation, such as electrode passivation or dendrite formation (FIG. 4). We believe that our insights into capacity loss are representative of the field and are intended as guidance for continued advancement and innovation in this field.

Electrolytes contain redox species, supporting salts and solvents, but when considering capacity loss, it is the chemical decomposition of the redox species that must be considered first (FIG. 4b). Good chemical stability is the key advantage of most inorganic species. However, some transition metal species, such as  $\text{Fe}^{3+}/\text{Fe}^{2+}$ , are

known to precipitate during long-duration testing as a result of hydrolysis. Capacity decay in aqueous organic RFBs is most often a result of decomposition that can occur through various mechanisms<sup>140</sup>, including nucleophilic substitution/Michael addition, hydrolysis, disproportionation, dimerization, tautomerization and desulfonation<sup>98</sup> (BOX 3). In addition to the intrinsic instability of redox species, the solvent and supporting salt may also play roles in capacity loss. For example, water splitting is a typical side reaction in aqueous systems, with the evolution of hydrogen and oxygen causing many subsequent problems. By comparison, the variety of organic solvents available for non-aqueous systems increases the complexity of solvent-dependent side reactions<sup>67</sup>, which are far less well understood. Some organic radicals generated during the charging and discharging are sensitive to environmental conditions<sup>74</sup> (that is, oxygen, temperature, light) or the purity of solvents (that is,  $\text{H}_2\text{O}$ ), resulting in undesirable decay. Another intrinsic instability of redox species is the large solubility change between their oxidized and reduced states. Because the chemical decomposition is the intrinsic instability, adopting functional additives to suppress

### Regeneration

The recovery of active species after crossover without sacrificing capacity, which is similar to rebalancing.

### Symmetric cell

A symmetric cell uses the same redox species (but exploits different oxidation states) on both sides of the cell. In the unbalanced configuration, using excess charge for the counter electrolyte minimizes its negative impact on the cell capacity decay.

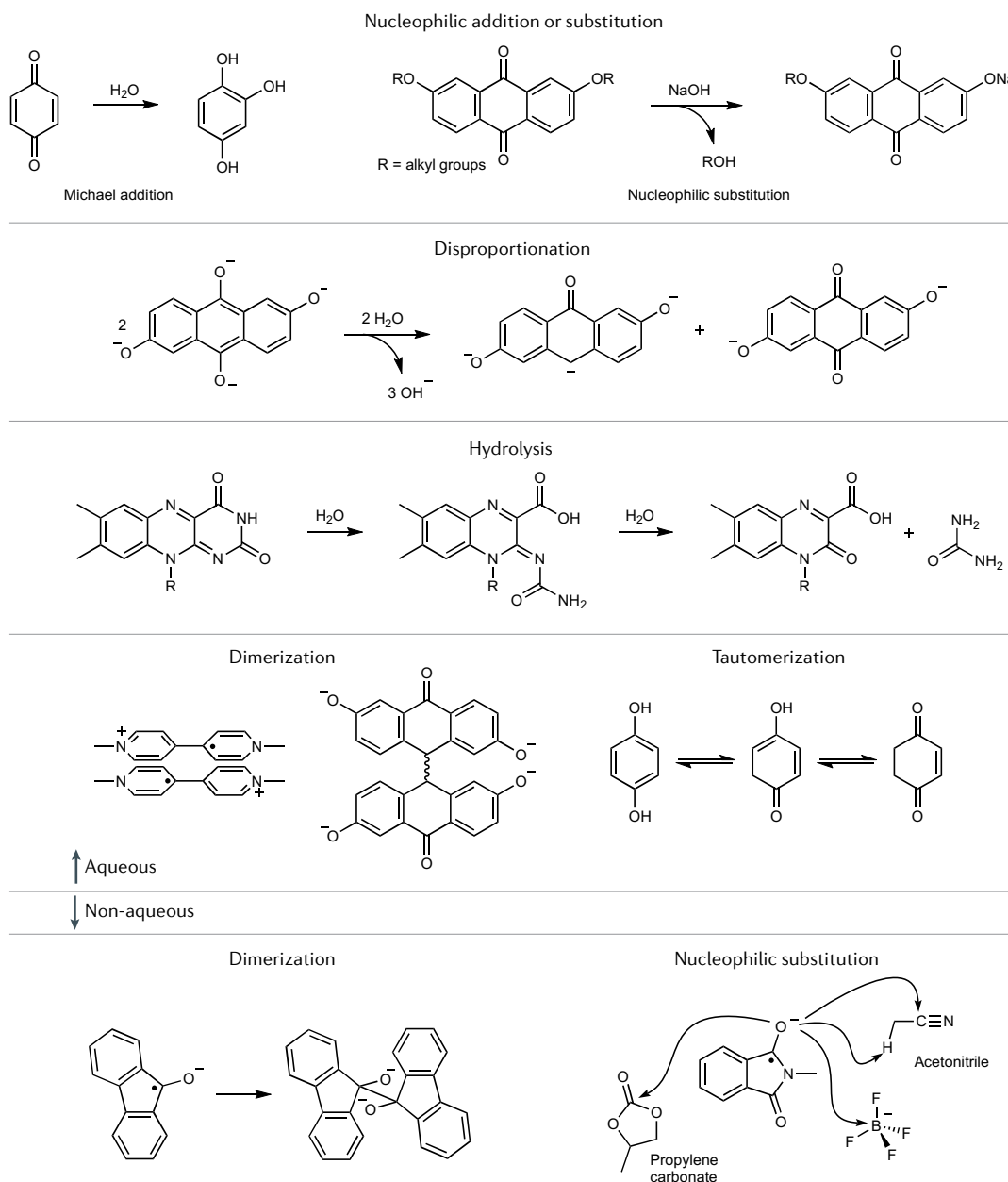
hydrolysis or water splitting or exploiting molecular engineering to improve stability and solubility are likely to be more effective than revising testing strategies for mitigating capacity decay. Decomposition phenomena are also dependent on both concentration and time; thus, these must be taken into account when assessing the capacity fade rate.

Membrane crossover issues (FIG. 4c) differ with the types of membranes and redox species<sup>144</sup>. In aqueous systems, the principally adopted separators are selectively ion-conductive membranes. The main working principles are either charge or size exclusion<sup>145</sup>. In general, organic molecules display lower membrane permeability than metal ions as a result of their larger

size<sup>146</sup>. Crossover represents one of the most critical challenges for traditional aqueous RFBs using metal-based redox species, such as vanadium flow batteries<sup>16,147</sup>. Although regeneration can eliminate the crossover effect for vanadium-based redox species, low efficiency and high cost of replacing decayed electrolytes may harm the widespread implementation of RFBs. Perfect membrane selectivity is challenging to achieve even for organic molecules, so a combination of symmetric cell and asymmetric cell tests are usually used to evaluate the stability of new organic species, while the unbalanced symmetric configuration may be helpful to determine the chemical degradation rate of redox-active molecules<sup>136,148</sup>. For non-aqueous RFBs,

### Box 3 | Illustration of key chemical degradation mechanisms of redox-active molecules

We present the main chemical degradation widely mentioned in the study of redox flow batteries.



## Asymmetric cell

The asymmetric full-cell configuration uses different active materials with suitable potential difference in the catholyte and the anolyte, respectively. In a charge-unbalanced cell, one is the working electrolyte (limited charge) and the other serves as the counter electrolyte (excess charge).

porous membranes are frequently used for performance demonstration as a result of their good chemical stability in diverse organic solvents<sup>130</sup>. Crossover is unavoidable, but its impact can be reduced by applying the symmetric full-cell concept, using the same mixed electrolyte including both positive and negative species<sup>113</sup>. However, relatively low Coulombic efficiencies (90–95%) are typically observed in non-aqueous RFB demonstrations (99% would be considered high efficiency). A symmetric full-cell design can also be achieved by adopting bipolar or biredox molecules, such as 2-phenyl-4,4,5,5-tetramethylimidazoline-1-oxyl-3-oxide<sup>100</sup>, TEMPO/phenazine combi-molecule<sup>134</sup> or methyl viologen dibromide<sup>149</sup>, which can each undergo reversible reactions at both the positive and the negative electrodes. With the same redox species used as both catholyte and anolyte, such a setup may better mitigate the influence of crossover. Crossover can also be affected by the concentration of redox species, membrane type and thickness, applied current density, electrolyte volume and electrode area. Thus, for firm conclusions to be drawn, it is essential that comparisons are made under consistent experimental conditions. Moreover, it has been suggested that a solid ceramic membrane can completely prevent crossover, and, thus, be beneficial in studying the intrinsic stability of redox species, albeit that the applied current density is limited as a result of low ionic conductivity<sup>12</sup>. It should also be noted that solid ceramic membranes are pH-sensitive and can only be applied in a limited potential range. Finally, they are not easy to handle, owing to poor mechanical properties.

Capacity loss can also be associated with electrode passivation and membrane degradation, both of which can lead to an increase of internal resistance. The voltage is strongly correlated with internal resistance, this in turn severely increases the overpotential between charging and discharging and, thus, decreases the cycling capacity that can be delivered at the fixed cut-off voltages. Some reports have proposed galvanostatic testing with a potentiostatic hold at the end of each charging and discharging step in order to accurately assess the long-term stability of organic molecules by isolating the true capacity fade rate<sup>140</sup>. In hybrid RFBs, the metal anode typically displays dendrite formation (such as Zn or Li dendrites) during repeated stripping and deposition. For aqueous Zn-based flow batteries, the relatively low Coulombic efficiency is a typical feature that accompanies the depletion of Zn, resulting in a sudden decay in capacity when dendrites accumulate. In batteries with solid membranes, Li dendrite formation can lead to cracks in the membrane and, thus, induce crossover. Refreshing the metal electrode can help to regenerate the capacity with an improved Coulombic efficiency.

## Applied characterizations

As with Li-ion batteries, advanced (for example, in situ) characterizations are crucial for studying the electrochemical properties of redox-active materials and understanding the mechanisms that underlie their operation and degradation. Only with a comprehensive understanding of reaction mechanisms and cycling stability will it be possible to develop general guidelines for

the rational design of redox-active materials for RFBs. Improved characterization methods are needed to enhance the performance and extend the battery life of both organic-based and inorganic-based systems. Redox reactions generally occur in liquid electrolytes for RFBs, and, thus, spectroscopic characterization methods are preferred for mechanistic studies. So far, methods such as optical spectrophotometry (ultraviolet–visible (UV–Vis), Fourier transform infrared and Raman spectroscopy), nuclear magnetic resonance (NMR), mass spectrometry and electron paramagnetic resonance (EPR) spectroscopy have been used to study the underlying mechanisms of organic molecules in RFBs. In general, the in situ/operando characterizations are more encouraged to have a deep and comprehensive understanding of mechanisms underlying the redox chemistries.

**Ex situ spectroscopic analysis.** EPR is an ideal method to detect the radical species present during battery charging and discharging. A state of charge (SOC) estimation method that relies on EPR was reported by Wang and colleagues<sup>78</sup> (FIG. 5a).

During the charging process of a flow battery containing 0.5 M TEMPO, 50- $\mu$ L aliquots of electrolyte were extracted at various times and subjected to EPR analysis in order to measure the concentration of neutral TEMPO radical. Both the derived TEMPO concentration and the battery SOC exhibited a linear correlation with battery charging time, thus providing an effective tool to estimate SOC in a Li-TEMPO flow battery. The method is anticipated to be effective for other radical species involved in the operation of RFBs. In addition to SOC and battery health monitoring through EPR, this technique is also useful for the investigation of the redox process intermediates and redox mechanism. For example, it has been applied to characterize and quantify the fluorenone radical anion intermediates in an aqueous RFB that relies on ketone hydrogenation and dehydrogenation<sup>98</sup>. By quantitatively determining the radical concentration, a unique chemical-reaction-involved battery cycling process can be confirmed.

UV-vis spectroscopy is also a straightforward tool that can be used to determine molecular structure changes during battery cycling. For instance, in the first report describing the use of azobenzenes in RFBs by Yu and colleagues, UV-vis analysis was used to reveal where the redox centre resided<sup>92</sup> (FIG. 5b). Once discharged, the characteristic peak from phenyl regions exhibited a significant blue shift owing to an electron density change around the central N=N bond. The changes in the azo group n- $\pi^*$  absorption could also be observed periodically throughout charging–discharging cycles.

Electrolytes based on deep eutectic solvents have become appealing for their high concentration of active species and high energy density. Raman spectroscopy is useful in detecting the interaction between the components of an eutectic electrolyte. For example, in the iron-based eutectic electrolyte reported by Yu and colleagues, clear changes could be observed in the Raman peak for [FeCl<sub>4</sub>]<sup>-</sup> vibration when different molar ratios of the ethylene glycol additive were present<sup>120</sup> (FIG. 5c).



This was attributed to dissociation of  $[\text{FeCl}_4]^-$  in the presence of a large amount of ethylene glycol. The information obtained from Raman spectra can, thus, be used to guide optimization of electrolyte compositions.

NMR spectroscopy has been established as a direct powerful characterization technique for organic molecules used in organic RFBs. In a report describing organosulfur-based RFBs<sup>91</sup>,  $^{13}\text{C}$  NMR was applied to

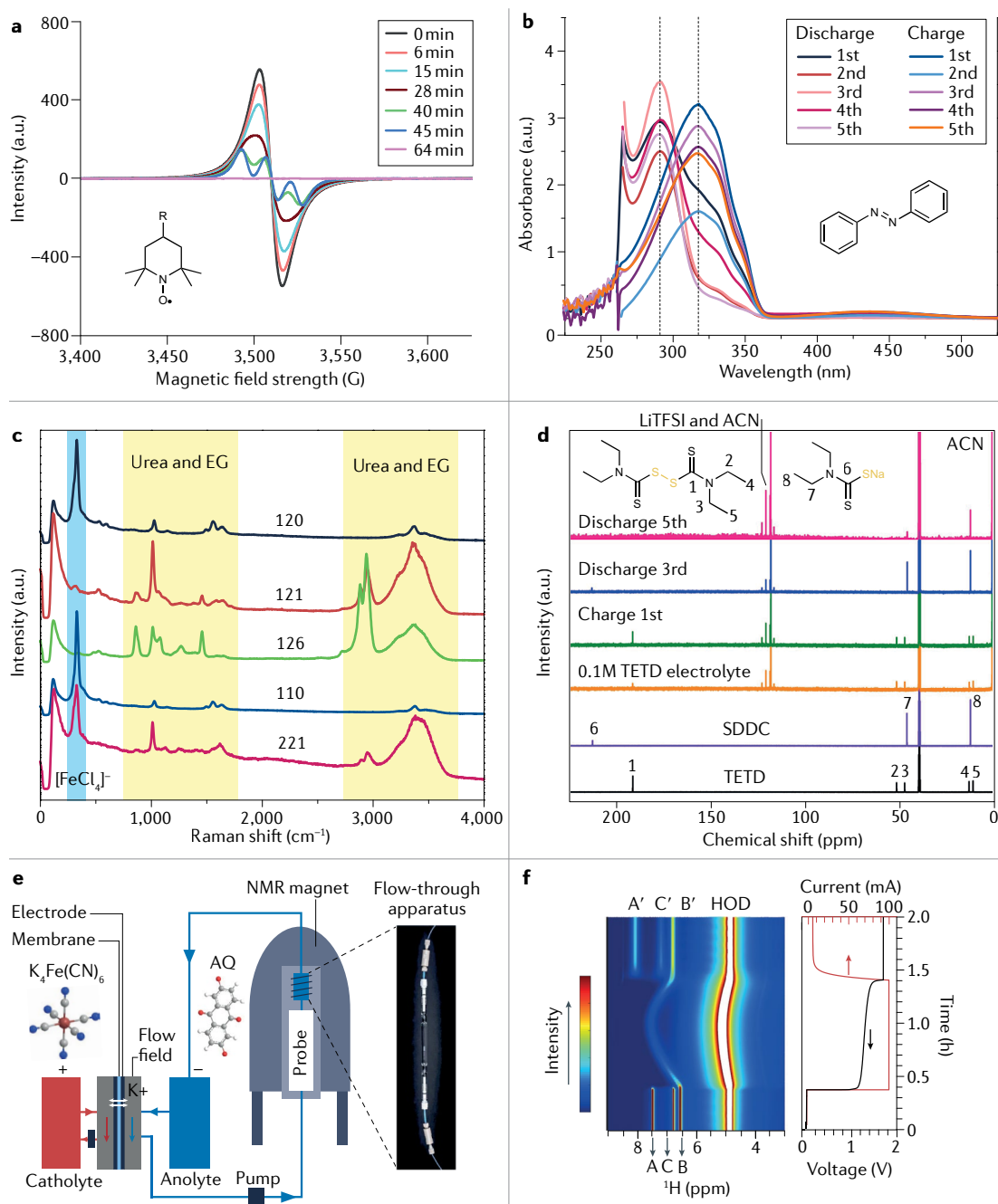


**Fig. 5 | Spectroscopic characterizations for understanding the materials chemistry.** **a** | Electron paramagnetic resonance (EPR) spectroscopy to detect the free radicals present in the 2,2,6,6-tetramethylpiperidine-1-oxyl species. **b** | Ultraviolet-visible spectroscopy to measure the oxidized/reduced species of azobenzene during charging and discharging. **c** | Raman spectroscopy to reveal the working mechanism of Fe-based deep eutectic solvents. **d** |  $^{13}\text{C}$  nuclear magnetic resonance (NMR) spectroscopy to investigate the reaction mechanism of organosulfur compounds. **e** | Schematic illustration of the NMR setup for in situ characterizations. **f** | In situ pseudo-2D  $^1\text{H}$  NMR spectroscopy to reveal the reaction mechanism and electrolyte decomposition of anthraquinone species in aqueous systems. ACN, acetonitrile; EG, ethylene glycol; LiTFSI, lithium bis(trifluoromethanesulfonyl)imide; SDDC, sodium diethyldithiocarbamate; TETD, tetraethylthiuram disulfide. Panel **a** adapted with permission from REF.<sup>78</sup>, Wiley. Panel **b** adapted with permission from REF.<sup>92</sup>, Springer Nature Ltd. Panel **c** adapted with permission from REF.<sup>120</sup>, Elsevier. Panel **d** adapted with permission from REF.<sup>91</sup>, Wiley. Panels **e** and **f** adapted with permission from REF.<sup>150</sup>, Springer Nature Ltd.

confirm the molecular structure of the charged species and the stability of the material during cycling (FIG. 5d).

**In situ characterization.** In situ characterization techniques are essential in revealing redox reaction mechanisms in play during battery operation. Recently, a delicate yet effective in situ NMR analysis technique was reported by Grey and colleagues<sup>150</sup> (FIG. 5e). An anthraquinone (DHAQ<sup>2-</sup>)-ferrocyanide RFB was employed as a model system. An in situ pseudo-2D <sup>1</sup>H NMR can be acquired as a function of charging time (FIG. 5f). Upon charging, the signal of the two ortho-position protons A and C diminished immediately due to electron delocalization, while the m-position proton B peak broadened and shifted downfield. As charging continued, the proton B peak signal reached a maximum chemical shift before narrowing and moving upfield as the semiquinones were further reduced. When the cell voltage was held at 1.7 V for potentiostatic charging, the final two-electron reduced product DHAQ<sup>4-</sup> proton signal was observed. During charging, the loss of signals for protons A and C suggested a rapid intermolecular electron transfer process between diamagnetic and paramagnetic ions. Variable-temperature experiments enabled the exchange transfer rate constant to be determined and the charging mechanism described quantitatively. DHA<sup>3-</sup> was confirmed to be the decomposed product after charging.

**Other characterizations.** A direct in situ visualization using fluorescence microscopy enabled mapping of the redox-active material and its reaction and transport within porous carbon electrodes<sup>151</sup>. Paired with electrochemical polarization, such a fluorescence map can provide valuable information for future electrode engineering, leading to better battery performance. Non-invasive battery health status monitoring is both convenient and appealing to researchers, especially in industrial applications. An acoustic approach to monitor vanadium RFB SOC was reported by Deng, Wang and colleagues, who measured the acoustic attenuation coefficient in situ and non-invasively<sup>152</sup>. The method proved to be highly successful, offering accurate measurement and low sensitivity to temperature when compared with the benchmark-inference method.

### Computational efforts in RFB design

Computational modelling is critically important for RFB research, as it can be used to investigate the intrinsic properties of molecular compounds and corresponding interactions in the electrolyte. It also helps to screen new organic redox species efficiently (redox potential, solubility). Calculations can provide detailed information about the molecular structure (stability and potential interactions) in the electrolyte and the effect of electrolytes and electrodes on the redox reaction. Computational high-throughput screening strategies can provide guidance to accelerate the search for redox species suitable for high-energy-power and low-cost RFB systems.

**Simulation-oriented materials design.** Theoretical simulations often facilitate the rational design of redox-active materials. By virtual screening using density functional

theory (DFT) simulations, the addition of electron-withdrawing and electron-donating groups onto alloxazine core structures can lead to variation of the operating potential of 400 mV (REF.<sup>104</sup>) (FIG. 6a). To give a specific example, a hydroxyl-functionalized alloxazine derivative increases the cell voltage by 10% compared with a carboxylic-acid-functionalized alloxazine, which, in turn, translates to 10% higher energy density.

As noted on several occasions in this Review, the solubility of redox-active materials is a key factor in determining battery energy density. Although material solubility can not yet be reliably predicted, calculating the molecule solvation energy using DFT study can provide a useful model of solubility trends. For example, Wei, Wang and colleagues reported that phenazines with carboxylate and sulfonate functional groups exhibited the highest solvation energy (FIG. 6b), suggesting that they would exhibit the highest solubility<sup>86</sup>. DHPS was selected as the anolyte material, delivering a capacity of 67 Ah l<sup>-1</sup> and capacity retention of 90% over 500 cycles. Ferrocyanide has been employed as a battery catholyte owing to its long lifetime in water. However, it suffers from relatively low solubility when compared with its counterpart anolyte. By modifying the coordination ligand with the earth-abundant iron centre, a recent report demonstrated superior material stability and high solubility in pH-neutral conditions<sup>105</sup>. Guided by Carnelley's rule, which states that a low symmetry analogue shows a higher solubility than analogues with a high symmetry, a symmetry-breaking design of iron(II)-bipyridine complex was proposed to increase molecular solubility. With the aid of ab initio molecular dynamics calculations, the detailed solvation structure of Na<sub>4</sub>[Fe<sup>II</sup>(Dcbpy)<sub>2</sub>(CN)<sub>2</sub>] can be revealed (FIG. 6c). As indicated by critical radial distribution functions, the peak of  $\gamma_{\text{Fe-CO}_2}$  appeared at 7.0 Å, which is larger than [Fe(CN)<sub>6</sub>]<sup>4-</sup> (4.6 Å) and [Fe(bpy)]<sup>2+</sup> (6.3 Å). A broad distribution of the Fe-O<sub>water</sub> peak from a classical molecular dynamics simulation also suggested a non-spherical shape of the hydration shell, supporting the symmetry-breaking design.

Material stability is an essential indicator in the evaluation of a RFB material. A powerful tool enabling quantitative prediction of radical lifetime in charged pyridinium-based anolytes was reported by Minter, Sigman, Sanford and colleagues<sup>153</sup> (FIG. 6d). DFT-based virtual screening and experimental validation of 16 pyridinium-derived radical compounds showed that *N*-xylyl-substituted pyridinium-derived radicals are theoretically three orders of magnitude more stable than simple methyl-substituted pyridinium-derived radicals. Single-crystal X-ray analysis showed that, in an *N*-xylyl-substituted pyridinium-derived radical, the perpendicular xylyl substituent protects the C2/C6 position, preventing homocoupling of the radical species. This observation aligned well with the MV-derived battery material decomposition mechanism.

**Reaction mechanism understanding.** Computational simulations can be useful to achieve deeper insights into the reaction mechanisms. Combined with experimental results, they can help to reveal more clearly the

mechanisms underlying the properties of redox-active molecules. For example, Zhao, Yu and colleagues used DFT analysis<sup>87</sup> to calculate the lowest unoccupied molecular orbital and highest occupied molecular orbital of the MB molecule and suggest that it is structurally stable as a result of effective electron delocalization and conjugation (FIG. 6e). The difference in energy between the highest occupied molecular orbitals of MB and its possible reduced state can help to indicate which reaction pathway might occur most easily. FIGURE 6f shows the nucleus-independent chemical shift and anisotropy of the induced current density (ACID) calculations, in which ACID is a magnetic indicator of aromaticity for visualizing ring currents and electron delocalization, which can be applied to provide understanding of the redox mechanism of MB. Providing a visualization of ring currents and electron delocalization, the ACID plot gives results consistent with the nucleus-independent

chemical shift calculation, confirming the reversal of aromaticity of the thiazine ring (from aromatic to antiaromatic) and strong aromaticity of benzenoid rings upon the reduction of MB. In addition, a good match between voltage profile and simulated voltages can suggest the possible reaction steps as well as potential cation/anion coordination.

### Conclusion and outlook

New materials chemistry promises the development of the next generation of green, long-life and high-energy RFBs. Despite numerous recent advancements, improved experimental performances have yet to result in improvements at the practical level. More comprehensive studies that integrate electrolyte design and advanced characterization are essential for in-depth understanding of battery capacity, decay mechanisms and performance. In this section, we summarize the

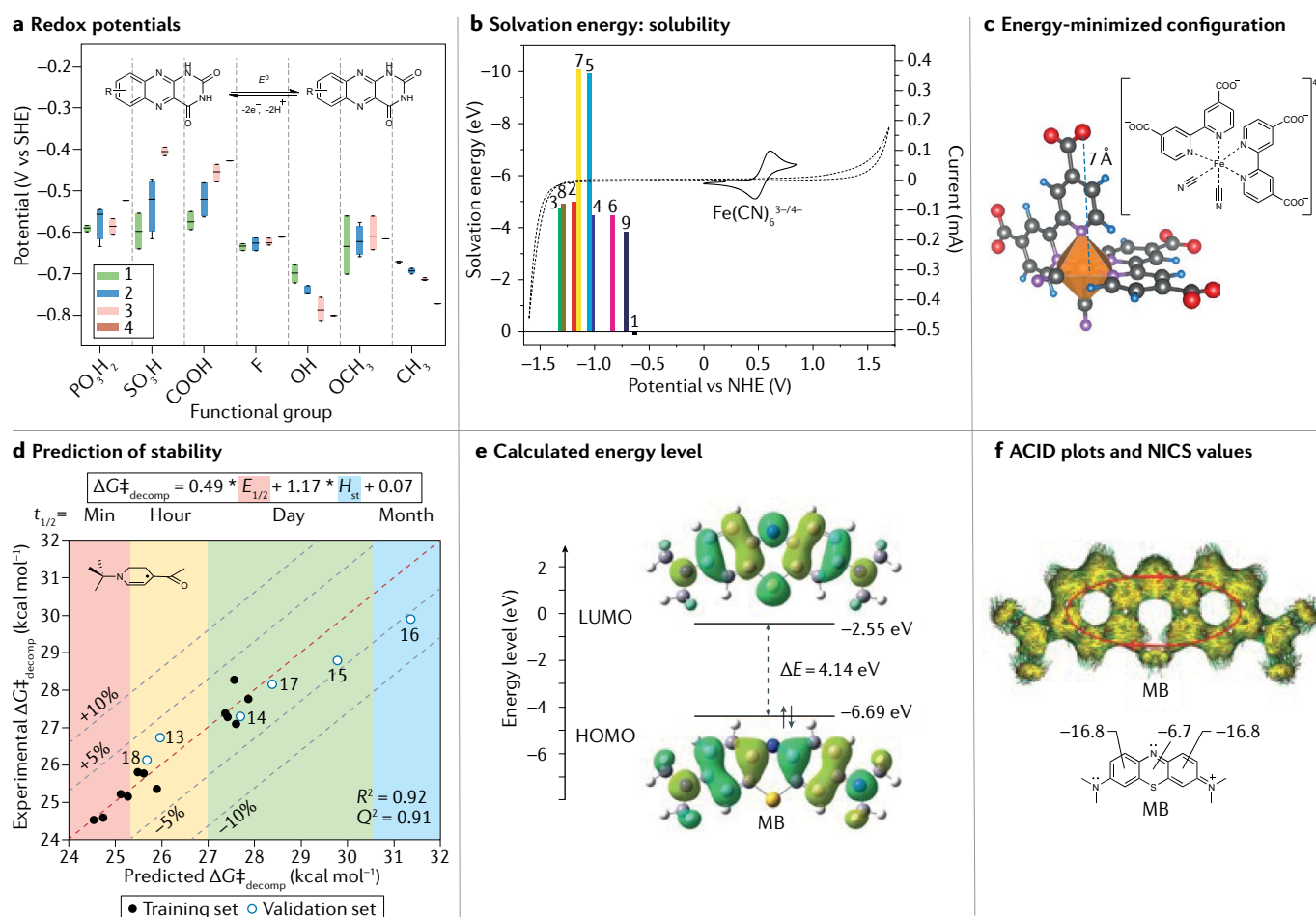


**Fig. 6 | Computational study to understand and guide rational designs of redox-active molecules.** **a** | Computationally predicted redox potentials of alloxazine derivatives based on the type of functional groups and substituted numbers. **b** | Solvation energy calculation of phenazine derivatives to predict the solubility. **c** | Energy-minimized configuration simulated to understand the influence of coordinated ligands on the solvation structure of organometallic materials. **d** | Prediction of electrochemical stability of pyridinium species based on a predictive model using electronic and steric parameters. **e** | Optimized structure and calculated energy levels of methylene blue (MB) molecules to understand

electrochemical properties, including electronic stability and electron transfer. **f** | The nucleus-independent chemical shift (NICS) and anisotropy of the induced current density (ACID) calculations for understanding redox chemistry. HOMO, highest occupied molecular orbital; LUMO, lowest unoccupied molecular orbital; NHE, normal hydrogen electrode. Panel **a** adapted with permission from REF.<sup>104</sup>, Springer Nature Ltd. Panel **b** adapted with permission from REF.<sup>86</sup>, Springer Nature Ltd. Panel **c** adapted with permission from REF.<sup>105</sup>, Springer Nature Ltd. Panel **d** adapted with permission from REF.<sup>153</sup>, ACS. Panels **e** and **f** adapted with permission from REF.<sup>87</sup>, Wiley.

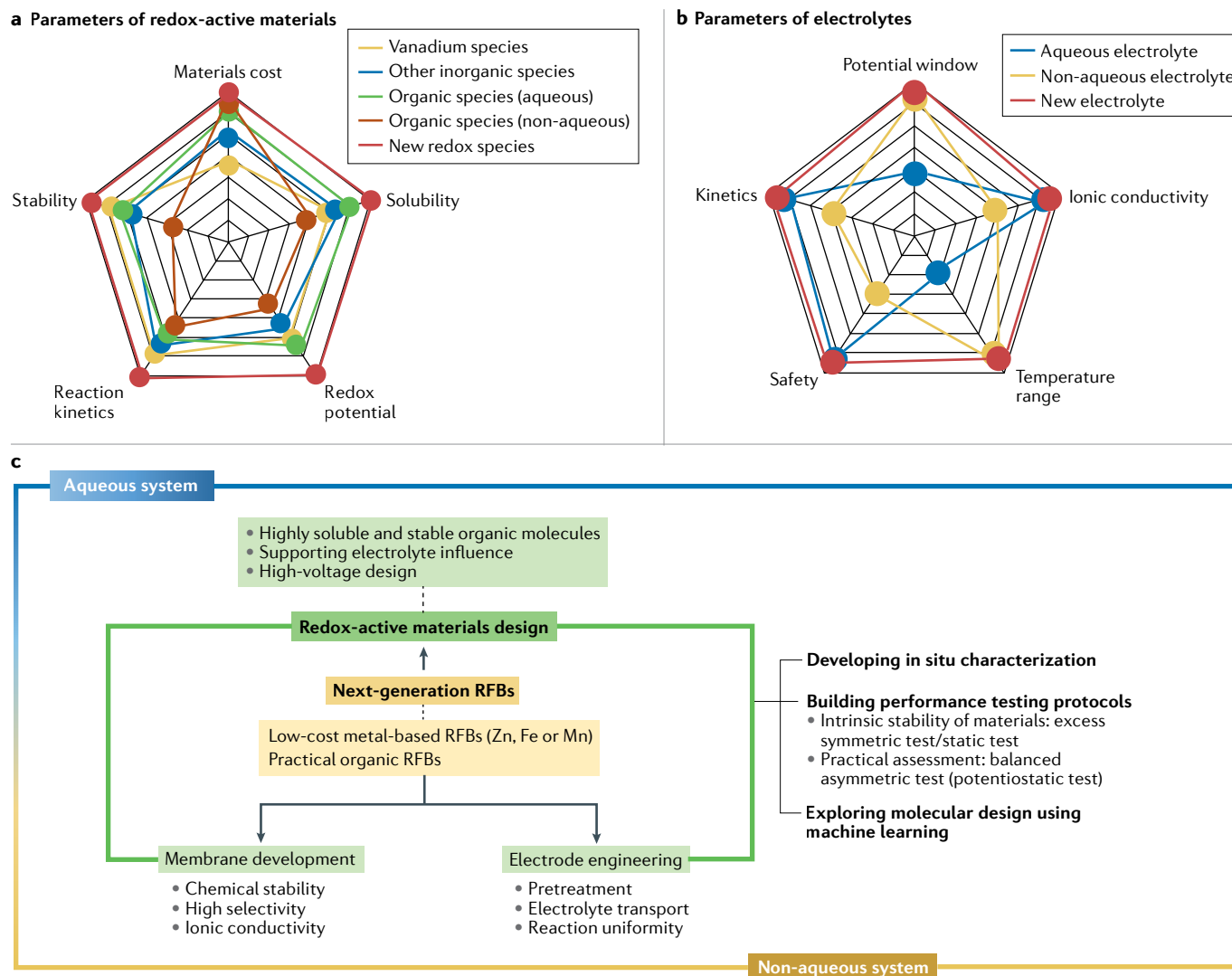


Fig. 7 | **Future prospects for the development of next-generation RFBs.** **a** | Required parameters for promising redox-active materials. **b** | Required parameters for promising electrolytes. **c** | Perspective on future developments of next-generation flow battery technologies. RFB, redox flow battery.

emerging materials chemistry and the key parameters, the remaining issues and potential avenues to achieve next-generation RFBs. Finally, we provide our thoughts on the design criteria that must be followed in order to enable sustainable, long-duration and high-performance energy storage systems.

Conventional RFB designs have focused on developing promising redox chemistries with features of high concentration, long-term stability, suitable redox potential and cost-effectiveness (FIG. 7a). Although many favourable organic redox-active materials have been designed for aqueous RFBs, most of them are demonstrated only at a limited concentration (less than 0.5 M), and the achieved capacity fade rate (1–10% per day) does not meet the stability requirement for practical applications. Some advanced organic molecules have been reported to show a low capacity fade rate (<0.02% per day), which approaches a practical standard, but this performance is demonstrated in unbalanced cell tests using excess counter electrolytes. Many molecular species employed

in RFBs are suitable for use only in an isolated pH value range, such as strongly acidic or alkaline electrolytes. As a result, pairing organic molecules with the large difference in redox potentials to realize high-voltage, high-energy and stable aqueous RFBs remains challenging. As it stands, only a few aqueous all-organic-based RFBs have been demonstrated, showing a relatively low working voltage (1–1.2 V), and with long-term stability reported using cell tests with an oversized counter electrolyte to isolate the influence of the counter electrolyte on the overall cell capacity performance.

For non-aqueous systems, some highly soluble organic molecules have been found, showing a concentration more than 2 M, whereas most of the demonstrated cycling properties are based on a low concentration (0.1 M), not to mention the limited chemical stability and reaction kinetics in organic solvents. Moreover, for the practical use of non-aqueous systems, it is important to design a sealing system with inert gas protection in order to minimize the influence of moisture and oxygen.

Although challenging, this is not insurmountable, as it is arguably more manageable than the tightly controlled conditions in the semiconductor industry or in the typical organic synthesis employed for pharmaceutical manufacture. Furthermore, although non-aqueous electrolytes can provide a wide potential window, high-voltage flow battery designs remain less well developed owing to the narrow potential separation of the reported redox species. In addition, for many common organic solvents, flammability and the limitations imposed by their physical properties hamper the development of practical systems (FIG. 7b). For redox-targeting or solar flow batteries, in addition to redox species, the technical challenge is to achieve optimal matching between redox species and solid active materials or semiconductor photoelectrodes, respectively. Given the working principle and performance metrics, the difficulty of engineering compact installations and the limited power density are obstacles for practical large-scale implementation of solar or semi-solid RFBs. The cost of such systems is also a concern. For a practical solar RFB design, commercially viable silicon-based solar cells may be cost-effective and efficient candidates.

Many challenges remain for the realization of next-generation RFBs, from the development of single materials to practical device demonstration, including the molecular design, membrane innovation and electrode engineering (FIG. 7c). However, through a comprehensive consideration of performance metrics, cost and sustainability, Zn-based or all-organic-based flow batteries may have great potential for grid-scale energy storage. In terms of molecular design, any approach to finding promising organic molecules must focus first on high solubility and long-term chemical stability. From a practical viewpoint, the capacity fade rate of organic RFBs must be demonstrated at a reasonably high concentration (>1 M), because, in addition to the initial material cost, the costs of periodic replacement will increase the overall capital cost. The effect of solvents and supporting salts on the redox chemistry (and also an evaluation of their cost) must also be taken into consideration,

especially for non-aqueous systems. For reference, the capital costs of vanadium-based RFBs are frequently quoted in the range of \$300–600 per kWh. The US Department of Energy Office of Electricity has targeted a cost for future RFBs of no more than \$150 per kWh to be commercially feasible, while \$100 per kWh is more desirable for widespread penetration<sup>68</sup>. The general principles in reducing the cost are to design high-performance yet low-cost raw materials including redox-active materials and membranes, while improving the lifetime to minimize replacement costs. Second, it is important to explore organic molecules with low or high redox potentials to enable high-voltage RFBs (3 V), and, thus, take full advantage of the wide potential window of non-aqueous electrolytes<sup>154</sup>. Third, new low-cost ion-conductive membranes with considerable conductivity and high selectivity need to be realized. In addition, the rational engineering of electrodes combined with a comprehensive understanding of the redox mechanisms inside porous carbon materials will be essential for improving performance. Fourth, although some decay mechanisms have been proposed for organic molecules, more in situ and real-time characterizations on the reaction chemistry will provide further insights into the underlying mechanisms associated with electron transfer. Meanwhile, standard performance testing methods should be developed to access the promise of organic active materials under practical conditions. In addition, computational modelling, including machine learning, will significantly impact the design of new molecules, as well as helping to develop structure–property relationships. In targeting these aspects, we hope to inspire the research community to further advance flow battery chemistry and move the technology from the realm of fundamental science to practical systems. We argue that systematic comparison of different electrochemical energy storage systems should be reserved until they are at similarly mature stages of development.

Published online 17 June 2022

1. Van Noorden, R. The rechargeable revolution: a better battery. *Nature* **507**, 26–28 (2014).
2. Dunn, B., Kamath, H. & Tarascon, J.-M. Electrical energy storage for the grid: a battery of choices. *Science* **334**, 928–935 (2011).
3. Choi, J. W. & Aurbach, D. Promise and reality of post-lithium-ion batteries with high energy densities. *Nat. Rev. Mater.* **1**, 16013 (2016).
4. Yang, Z. et al. Electrochemical energy storage for green grid. *Chem. Rev.* **111**, 3577–3613 (2011).
5. Li, B. & Liu, J. Progress and directions in low-cost redox-flow batteries for large-scale energy storage. *Nat. Sci. Rev.* **4**, 91–105 (2017).
6. Dowling, J. A. et al. Role of long-duration energy storage in variable renewable electricity systems. *Joule* **4**, 1907–1928 (2020).
7. Sepulveda, N. A., Jenkins, J. D., Edington, A., Mallapragada, D. S. & Lester, R. K. The design space for long-duration energy storage in decarbonized power systems. *Nat. Energy* **6**, 506–516 (2021).
8. Hunter, C. A. et al. Techno-economic analysis of long-duration energy storage and flexible power generation technologies to support high-variable renewable energy grids. *Joule* **5**, 2077–2101 (2021).
9. Soloveichik, G. L. Flow batteries: current status and trends. *Chem. Rev.* **115**, 11533–11558 (2015).
10. Park, M., Ryu, J., Wang, W. & Cho, J. Material design and engineering of next-generation flow-battery technologies. *Nat. Rev. Mater.* **2**, 16080 (2017).
11. Wang, Y., He, P. & Zhou, H. Li-redox flow batteries based on hybrid electrolytes: at the cross road between Li-ion and redox flow batteries. *Adv. Energy Mater.* **2**, 770–779 (2012).
12. Zhao, Y. et al. A chemistry and material perspective on lithium redox flow batteries towards high-density electrical energy storage. *Chem. Soc. Rev.* **44**, 7968–7996 (2015).
13. Gong, K., Fang, Q., Gu, S., Li, S. F. Y. & Yan, Y. Nonaqueous redox-flow batteries: organic solvents, supporting electrolytes, and redox pairs. *Energy Environ. Sci.* **8**, 3515–3530 (2015).
14. Ding, Y., Zhang, C., Zhang, L., Zhou, Y. & Yu, G. Molecular engineering of organic electroactive materials for redox flow batteries. *Chem. Soc. Rev.* **47**, 69–103 (2018).
15. **A systematic overview of the development of redox-active organic materials for RFBs.**
16. Xiong, P., Zhang, L., Chen, Y., Peng, S. & Yu, G. A chemistry and microstructure perspective on ion-conducting membranes for redox flow batteries. *Angew. Chem. Int. Ed.* **60**, 24770–24798 (2021).
17. Li, X., Zhang, H., Mai, Z., Zhang, H. & Vankelcom, I. Ion exchange membranes for vanadium redox flow battery (VRB) applications. *Energy Environ. Sci.* **4**, 1147–1160 (2011).
18. Yuan, Z., Zhang, H. & Li, X. Ion conducting membranes for aqueous flow battery systems. *Chem. Commun.* **54**, 7570–7588 (2018).
19. Chen, D. et al. Polybenzimidazole membrane with dual proton transport channels for vanadium flow battery applications. *J. Membr. Sci.* **586**, 202–210 (2019).
20. Chen, D., Chen, X., Ding, L. & Li, X. Advanced acid-base blend ion exchange membranes with high performance for vanadium flow battery application. *J. Membr. Sci.* **553**, 25–31 (2018).
21. Peng, S. et al. Polybenzimidazole membranes with nanophase-separated structure induced by non-ionic hydrophilic side chains for vanadium flow batteries. *J. Mater. Chem. A* **6**, 3895–3905 (2018).
22. Shi, M. et al. Membranes with well-defined selective layer regulated by controlled solvent diffusion for high power density flow battery. *Adv. Energy Mater.* **10**, 2001382 (2020).
23. Dai, Q. et al. Thin-film composite membrane breaking the trade-off between conductivity and selectivity for a flow battery. *Nat. Commun.* **11**, 13 (2020).
24. Zhang, L. et al. Enabling graphene-oxide-based membranes for large-scale energy storage by controlling hydrophilic microstructures. *Chem* **4**, 1035–1046 (2018).
25. Baran, M. J. et al. Design rules for membranes from polymers of intrinsic microporosity for crossover-free aqueous electrochemical devices. *Joule* **3**, 2968–2985 (2019).
26. Tan, R. et al. Hydrophilic microporous membranes for selective ion separation and flow-battery energy storage. *Nat. Mater.* **19**, 195–202 (2020).



26. Zuo, P. et al. Sulfonated microporous polymer membranes with fast and selective ion transport for electrochemical energy conversion and storage. *Angew. Chem. Int. Ed.* **132**, 9651–9660 (2020).
27. Peng, S. et al. Gradient-distributed metal–organic framework-based porous membranes for nonaqueous redox flow batteries. *Adv. Energy Mater.* **8**, 1802533 (2018).
28. Yuan, J. et al. Membranes in non-aqueous redox flow battery: a review. *J. Power Sources* **500**, 229983 (2021).
29. Ke, X. et al. Rechargeable redox flow batteries: flow fields, stacks and design considerations. *Chem. Soc. Rev.* **47**, 8721–8743 (2018).
30. Jiang, H. et al. A high power density and long cycle life vanadium redox flow battery. *Energy Stor. Mater.* **24**, 529–540 (2020).
31. Mukhopadhyay, A. et al. Mass transfer and reaction kinetic enhanced electrode for high-performance aqueous flow batteries. *Adv. Funct. Mater.* **29**, 1903192 (2019).
32. Zhang, C. et al. Progress and prospects of next-generation redox flow batteries. *Energy Stor. Mater.* **15**, 324–350 (2018).
33. Ding, Y., Zhang, C., Zhang, L., Zhou, Y. & Yu, G. Pathways to widespread applications: development of redox flow batteries based on new chemistries. *Chem* **5**, 1964–1987 (2019).
34. Li, W. & Jin, S. Design principles and developments of integrated solar flow batteries. *Acc. Chem. Res.* **53**, 2611–2621 (2020).
35. Yan, R. & Wang, Q. Redox-targeting-based flow batteries for large-scale energy storage. *Adv. Mater.* **30**, 1802406 (2018).
36. Yuan, Z. et al. Advanced materials for zinc-based flow battery: development and challenge. *Adv. Mater.* **31**, 1902025 (2019).
37. Yuan, Z. et al. Negatively charged nanoporous membrane for a dendrite-free alkaline zinc-based flow battery with long cycle life. *Nat. Commun.* **9**, 3731 (2018).
38. Duduta, M. et al. Semi-solid lithium rechargeable flow battery. *Adv. Energy Mater.* **1**, 511–516 (2011).
39. Chen, H. et al. Sulphur-impregnated flow cathode to enable high-energy-density lithium flow batteries. *Nat. Commun.* **6**, 5877 (2015).
40. Ventosa, E., Amedu, O. & Schuhmann, W. Aqueous mixed-cation semi-solid hybrid-flow batteries. *ACS Appl. Energy Mater.* **1**, 5158–5162 (2018).
41. Jia, C. et al. High-energy density nonaqueous all redox flow lithium battery enabled with a polymeric membrane. *Sci. Adv.* **1**, e1500886 (2015).
42. Zhu, Y. G. et al. Unleashing the power and energy of LiFePO<sub>4</sub>-based redox flow lithium battery with a bifunctional redox mediator. *J. Am. Chem. Soc.* **139**, 6286–6289 (2017).
43. Chen, Y. et al. A stable and high-capacity redox targeting-based electrolyte for aqueous flow batteries. *Joule* **3**, 2255–2267 (2019).
44. Zhou, M. et al. Nernstian-potential-driven redox-targeting reactions of battery materials. *Chem* **3**, 1036–1049 (2017).
45. Zhou, Y. et al. Efficient solar energy harvesting and storage through a robust photocatalyst driving reversible redox reactions. *Adv. Mater.* **30**, 1802294 (2018).
46. Li, W. et al. High-performance solar flow battery powered by a perovskite/silicon tandem solar cell. *Nat. Mater.* **19**, 1326–1331 (2020).
47. Luo, J., Hu, B., Hu, M., Zhao, Y. & Liu, T. L. Status and prospects of organic redox flow batteries toward sustainable energy storage. *ACS Energy Lett.* **4**, 2220–2240 (2019).
48. Li, Z. & Lu, Y. C. Material design of aqueous redox flow batteries: fundamental challenges and mitigation strategies. *Adv. Mater.* **32**, 2002132 (2020).
49. Reale, E. R., Shrivastava, A. & Smith, K. C. Effect of conductive additives on the transport properties of porous flow-through electrodes with insulative particles and their optimization for Faradaic deionization. *Water Res.* **165**, 114995 (2019).
50. Murray, A. T., Voskian, S., Schreier, M., Hatton, T. A. & Surendranath, Y. Electrosynthesis of hydrogen peroxide by phase-transfer catalysis. *Joule* **3**, 2942–2954 (2019).
51. Wang, F. et al. Modular electrochemical synthesis using a redox reservoir paired with independent half-reactions. *Joule* **5**, 149–165 (2021).
52. Ren, S. et al. Molecular electrocatalysts can mediate fast, selective CO<sub>2</sub> reduction in a flow cell. *Science* **365**, 367–369 (2019).
53. Luo, J., Hu, B., Wu, W., Hu, M. & Liu, T. L. Nickel-catalyzed electrochemical C(sp<sup>3</sup>)–C(sp<sup>3</sup>) cross-coupling reactions of benzyl trifluoroborate and organic halides. *Angew. Chem. Int. Ed.* **60**, 6107–6116 (2021).
54. Mo, Y. et al. Microfluidic electrochemistry for single-electron transfer redox-neutral reactions. *Science* **368**, 1352–1357 (2020).
55. Novaes, L. F. T. et al. Electrocatalysis as an enabling technology for organic synthesis. *Chem. Soc. Rev.* **50**, 7941–8002 (2021).
56. Yan, M., Kawamata, Y. & Baran, P. S. Synthetic organic electrochemical methods since 2000: on the verge of a renaissance. *Chem. Rev.* **117**, 13230–13319 (2017).
57. Winsberg, J., Hagemann, T., Janoschka, T., Hager, M. D. & Schubert, U. S. Redox-flow batteries: from metals to organic redox-active materials. *Angew. Chem. Int. Ed.* **56**, 686–711 (2017).
58. Hnedkovsky, L., Wood, R. H. & Balashov, V. N. Electrical conductances of aqueous Na<sub>2</sub>SO<sub>4</sub>, H<sub>2</sub>SO<sub>4</sub>, and their mixtures: limiting equivalent ion conductances, dissociation constants, and speciation to 673 K and 28 MPa. *J. Phys. Chem. B* **109**, 9034–9046 (2005).
59. Su, L. et al. An investigation of the ionic conductivity and species crossover of lithiated nafion 117 in nonaqueous electrolytes. *J. Electrochem. Soc.* **163**, A5253 (2015).
60. Aaron, D. et al. Dramatic performance gains in vanadium redox flow batteries through modified cell architecture. *J. Power Sources* **206**, 450–453 (2012).
61. Suo, L. et al. “Water-in-salt” electrolyte enables high-voltage aqueous lithium-ion chemistries. *Science* **350**, 938–943 (2015).
62. Wang, W. et al. Recent progress in redox flow battery research and development. *Adv. Funct. Mater.* **23**, 970–986 (2013).
63. Zhang, L. & Yu, G. Hybrid electrolyte engineering enables safe and wide-temperature redox flow batteries. *Angew. Chem. Int. Ed.* **60**, 15028–15035 (2021).
64. Shin, S.-H., Yun, S.-H. & Moon, S.-H. A review of current developments in non-aqueous redox flow batteries: characterization of their membranes for design perspective. *RSC Adv.* **3**, 9095–9116 (2013).
65. Leung, P. et al. Recent developments in organic redox flow batteries: a critical review. *J. Power Sources* **360**, 243–283 (2017).
66. Xu, K. Nonaqueous liquid electrolytes for lithium-based rechargeable batteries. *Chem. Rev.* **104**, 4303–4418 (2004).
67. Wei, X. et al. Radical compatibility with nonaqueous electrolytes and its impact on an all-organic redox flow battery. *Angew. Chem. Int. Ed.* **54**, 8684–8687 (2015).
68. Darling, R. M., Gallagher, K. G., Kowalski, J. A., Ha, S. & Brushett, F. R. Pathways to low-cost electrochemical energy storage: a comparison of aqueous and nonaqueous flow batteries. *Energy Environ. Sci.* **7**, 3459–3477 (2014).
69. Zhao, Y. et al. A reversible Br<sub>2</sub>/Br<sup>−</sup> redox couple in the aqueous phase as a high-performance catholyte for alkaline batteries. *Energy Environ. Sci.* **7**, 1990–1995 (2014).
70. Zhao, Y., Wang, L. & Byon, H. R. High-performance rechargeable lithium-iodine batteries using triiodide/iodide redox couples in an aqueous cathode. *Nat. Commun.* **4**, 1896 (2013).
71. Chen, H. & Lu, Y.-C. A high-energy-density multiple redox semi-solid-liquid flow battery. *Adv. Energy Mater.* **6**, 1502183 (2016).
72. Xie, C., Duan, Y., Xu, W., Zhang, H. & Li, X. A low-cost neutral zinc–iron flow battery with high energy density for stationary energy storage. *Angew. Chem. Int. Ed.* **56**, 14953–14957 (2017).
73. Xie, C. et al. A highly reversible neutral zinc/manganese battery for stationary energy storage. *Energy Environ. Sci.* **13**, 135–143 (2020).
74. Wei, X. et al. Materials and systems for organic redox flow batteries: status and challenges. *ACS Energy Lett.* **2**, 2187–2204 (2017).
75. Ding, Y. & Yu, G. A bio-inspired, heavy-metal-free, dual-electrolyte liquid battery towards sustainable energy storage. *Angew. Chem. Int. Ed.* **55**, 4772–4776 (2016).
76. Lin, K. et al. Alkaline quinone flow battery. *Science* **349**, 1529–1532 (2015).
77. Huskinson, B. et al. A metal-free organic–inorganic aqueous flow battery. *Nature* **505**, 195–198 (2014).
78. Wei, X. et al. TEMPO-based catholyte for high-energy density nonaqueous redox flow batteries. *Adv. Mater.* **26**, 7649–7653 (2014).
79. Liu, T., Wei, X., Nie, Z., Sprenkle, V. & Wang, W. A total organic aqueous redox flow battery employing a low cost and sustainable methyl viologen anolyte and 4-HO-TEMPO catholyte. *Adv. Energy Mater.* **6**, 1501449 (2016).  
**One of the first demonstrations of an aqueous all-organic RFB.**
80. Janoschka, T., Martin, N., Hager, M. D. & Schubert, U. S. An aqueous redox-flow battery with high capacity and power: the TEMPTMA/MV system. *Angew. Chem. Int. Ed.* **55**, 14427–14430 (2016).
81. Hu, B., DeBruler, C., Rhodes, Z. & Liu, T. L. Long-cycling aqueous organic redox flow battery (AORFB) toward sustainable and safe energy storage. *J. Am. Chem. Soc.* **139**, 1207–1214 (2017).
82. DeBruler, C. et al. Designer two-electron storage viologen anolyte materials for neutral aqueous organic redox flow batteries. *Chem* **3**, 961–978 (2017).
83. Luo, J., Hu, B., Debruler, C. & Liu, T. L. A  $\pi$ -conjugation extended viologen as a two-electron storage anolyte for total organic aqueous redox flow batteries. *Angew. Chem. Int. Ed.* **57**, 231–235 (2018).
84. Milshtein, J. D. et al. High current density, long duration cycling of soluble organic active species for non-aqueous redox flow batteries. *Energy Environ. Sci.* **9**, 3531–3543 (2016).
85. Kowalski, J. A. et al. A stable two-electron-donating phenothiazine for application in nonaqueous redox flow batteries. *J. Mater. Chem. A* **5**, 24371–24379 (2017).
86. Hollas, A. et al. A biomimetic high-capacity phenazine-based anolyte for aqueous organic redox flow batteries. *Nat. Energy* **3**, 508–514 (2018).  
**An example of molecular engineering with screening of functional groups en route to a promising phenazine-based anolyte for aqueous RFBs.**
87. Zhang, C. et al. Phenothiazine-based organic catholyte for high-capacity and long-life aqueous redox flow batteries. *Adv. Mater.* **31**, e1901052 (2019).  
**Reports the use of phenothiazine derivative, MB, as a promising positive species in an acidic environment for aqueous RFBs.**
88. Kwon, G. et al. Bio-inspired molecular redesign of a multi-redox catholyte for high-energy non-aqueous organic redox flow batteries. *Chem* **5**, 2642–2656 (2019).
89. Kwon, G. et al. Multi-redox molecule for high-energy redox flow batteries. *Joule* **2**, 1771–1782 (2018).
90. Weng, C.-M. et al. Asymmetric allyl-activation of organosulfides for high-energy reversible redox flow batteries. *Energy Environ. Sci.* **12**, 2244–2252 (2019).
91. Zhang, L., Zhao, B., Zhang, C. & Yu, G. Insights into the redox chemistry of organosulfides towards stable molecule design in nonaqueous energy storage systems. *Angew. Chem. Int. Ed.* **60**, 4322–4328 (2021).
92. Zhang, L. et al. Reversible redox chemistry in azobenzene-based organic molecules for high-capacity and long-life nonaqueous redox flow batteries. *Nat. Commun.* **11**, 3843 (2020).  
**One of the first demonstrations of the reversible redox chemistry of azobenzene molecules for high-performance non-aqueous RFBs.**
93. Zu, X., Zhang, L., Qian, Y., Zhang, C. & Yu, G. Molecular engineering of azobenzene-based anolytes towards high-capacity aqueous redox flow batteries. *Angew. Chem. Int. Ed.* **59**, 22163–22170 (2020).
94. Sigel, H. & Martin, R. B. Coordinating properties of the amide bond. Stability and structure of metal ion complexes of peptides and related ligands. *Chem. Rev.* **82**, 385–426 (1982).
95. Häupler, B., Wild, A. & Schubert, U. S. Carbonyls: powerful organic materials for secondary batteries. *Adv. Energy Mater.* **5**, 1402034 (2015).
96. Ding, Y., Li, Y. & Yu, G. Exploring bio-inspired quinone-based organic redox flow batteries: a combined experimental and computational study. *Chem* **1**, 790–801 (2016).
97. Kwabi, D. G. et al. Alkaline quinone flow battery with long lifetime at pH 12. *Joule* **2**, 1894–1906 (2018).
98. Feng, R. et al. Reversible ketone hydrogenation and dehydrogenation for aqueous organic redox flow batteries. *Science* **372**, 836–840 (2021).  
**Introduces the idea of deprotonation to achieve reversible ketone reaction chemistry for aqueous RFBs.**
99. Liang, Y., Tao, Z. & Chen, J. Organic electrode materials for rechargeable lithium batteries. *Adv. Energy Mater.* **2**, 742–769 (2012).
100. Duan, W. et al. A symmetric organic-based nonaqueous redox flow battery and its state of

- charge diagnostics by FTIR. *J. Mater. Chem. A* **4**, 5448–5456 (2016).
101. Sinclair, N. S., Poe, D., Savinell, R. F., Maginn, E. J. & Wainright, J. S. A nitroxide containing organic molecule in a deep eutectic solvent for flow battery applications. *J. Electrochem. Soc.* **168**, 020527 (2021).
  102. DeBruin, C., Hu, B., Moss, J., Luo, J. & Liu, T. L. A sulfonate-functionalized viologen enabling neutral cation exchange, aqueous organic redox flow batteries toward renewable energy storage. *ACS Energy Lett.* **3**, 663–668 (2018).
  103. Orita, A., Verde, M. G., Sakai, M. & Meng, Y. S. A biomimetic redox flow battery based on flavin mononucleotide. *Nat. Commun.* **7**, 13230 (2016).
  104. Lin, K. et al. A redox-flow battery with an alloxazine-based organic electrolyte. *Nat. Energy* **1**, 16102 (2016).
  105. Li, X. et al. Symmetry-breaking design of an organic iron complex catholyte for a long cyclability aqueous organic redox flow battery. *Nat. Energy* **6**, 873–881 (2021).
  106. Zhao, Y. et al. Sustainable electrical energy storage through the ferrocene/ferrocenium redox reaction in aprotic electrolyte. *Angew. Chem. Int. Ed.* **126**, 11216–11220 (2014).
- One of the first demonstrations of reversible redox chemistry of organometallic molecules for non-aqueous RFBs.**
107. Wei, X. et al. Towards high-performance nonaqueous redox flow electrolyte via ionic modification of active species. *Adv. Energy Mater.* **5**, 1400678 (2015).
  108. Yu, J. et al. A robust anionic sulfonated ferrocene derivative for pH-neutral aqueous flow battery. *Energy Storage Mater.* **29**, 216–222 (2020).
  109. Cabrera, P. J. et al. Complexes containing redox noninnocent ligands for symmetric, multielectron transfer nonaqueous redox flow batteries. *J. Phys. Chem. C* **119**, 15882–15889 (2015).
  110. Sevov, C. S., Fisher, S. L., Thompson, L. T. & Sanford, M. S. Mechanism-based development of a low-potential, soluble, and cyclable multielectron anolyte for nonaqueous redox flow batteries. *J. Am. Chem. Soc.* **138**, 15378–15384 (2016).
  111. VanGelder, L. E., Pratt, H. D., Anderson, T. M. & Matson, E. M. Surface functionalization of polyoxovanadium clusters: generation of highly soluble charge carriers for nonaqueous energy storage. *Chem. Commun.* **55**, 12247–12250 (2019).
  112. Brushett, F. R., Vaughey, J. T. & Jansen, A. N. An all-organic non-aqueous lithium-ion redox flow battery. *Adv. Energy Mater.* **2**, 1390–1396 (2012).
  113. Duan, W. et al. “Wine-Dark Sea” in an organic flow battery: storing negative charge in 2,1,3-benzothiadiazole radicals leads to improved cyclability. *ACS Energy Lett.* **2**, 1156–1161 (2017).
  114. Huang, J. et al. Liquid catholyte molecules for nonaqueous redox flow batteries. *Adv. Energy Mater.* **5**, 1401782 (2015).
  115. Wang, G. et al. Exploring polycyclic aromatic hydrocarbons as an anolyte for nonaqueous redox flow batteries. *J. Mater. Chem. A* **6**, 13286–13293 (2018).
  116. Wei, X. et al. A high-current, stable nonaqueous organic redox flow battery. *ACS Energy Lett.* **1**, 705–711 (2016).
  117. Zhang, C., Zhang, L., Ding, Y., Guo, X. & Yu, G. Eutectic electrolytes for high-energy-density redox flow batteries. *ACS Energy Lett.* **3**, 2875–2883 (2018).
  118. Zhang, C., Zhang, L. & Yu, G. Eutectic electrolytes as a promising platform for next-generation electrochemical energy storage. *Acc. Chem. Res.* **53**, 1648–1659 (2020).
  119. Chen, J.-J., Symes, M. D. & Cronin, L. Highly reduced and protonated aqueous solutions of  $[P_2W_{18}O_{62}]^{6-}$  for on-demand hydrogen generation and energy storage. *Nat. Chem.* **10**, 1042–1047 (2018).
  120. Zhang, L., Zhang, C., Ding, Y., Ramirez-Meyers, K. & Yu, G. A low-cost and high-energy hybrid iron-aluminum liquid battery achieved by deep eutectic solvents. *Joule* **1**, 623–633 (2017).
- One of the first demonstrations of all-deep-eutectic-solvent-based flow batteries with coupling of the reaction of iron and aluminium.**
121. Zhang, C. et al. A sustainable redox-flow battery with an aluminum-based, deep-eutectic-solvent anolyte. *Angew. Chem. Int. Ed.* **56**, 7454–7459 (2017).
  122. Zhang, C. et al. Highly concentrated phthalimide-based anolytes for organic redox flow batteries with enhanced reversibility. *Chem* **4**, 2814–2825 (2018).
  123. Ding, Y. et al. Insights into hydrothermal solubilization for hybrid ion redox flow batteries. *ACS Energy Lett.* **3**, 2641–2648 (2018).
  124. Cong, G., Zhou, Y., Li, Z. & Lu, Y.-C. A highly concentrated catholyte enabled by a low-melting-point ferrocene derivative. *ACS Energy Lett.* **2**, 869–875 (2017).
  125. Shimizu, A. et al. Liquid quinones for solvent-free redox flow batteries. *Adv. Mater.* **29**, 1606592 (2017).
  126. VanGelder, L. E., Cook, T. R. & Matson, E. M. Progress in the design of polyoxovanadate-alkoxides as charge carriers for nonaqueous redox flow batteries. *Comments Inorg. Chem.* **39**, 51–89 (2019).
  127. Palmer, T. C. et al. A comparative review of metal-based charge carriers in nonaqueous flow batteries. *ChemSusChem* **14**, 1214–1228 (2021).
  128. Shrestha, A., Hendriks, K. H., Sigman, M. S., Minteer, S. D. & Sanford, M. S. Realization of an asymmetric non-aqueous redox flow battery through molecular design to minimize active species crossover and decomposition. *Chem. Eur. J.* **26**, 5369–5373 (2020).
  129. Tang, S. et al. Size effect of organosulfur and in situ formed oligomers enables high-utilization Na-organosulfur batteries. *Adv. Mater.* **33**, 2100824 (2021).
  130. Hendriks, K. H. et al. High-performance oligomeric catholytes for effective macromolecular separation in nonaqueous redox flow batteries. *ACS Cent. Sci.* **4**, 189–196 (2018).
  131. Janoschka, T. et al. An aqueous, polymer-based redox-flow battery using non-corrosive, safe, and low-cost materials. *Nature* **527**, 78–81 (2015).
  132. Burgess, M., Moore, J. S. & Rodriguez-López, J. Redox active polymers as soluble nanomaterials for energy storage. *Acc. Chem. Res.* **49**, 2649–2657 (2016).
  133. Winsberg, J. et al. Poly(TEMPO)/zinc hybrid-flow battery: a novel, “green,” high voltage, and safe energy storage system. *Adv. Mater.* **28**, 2238–2243 (2016).
  134. Winsberg, J. et al. TEMPO/phenazine combi-molecule: a redox-active material for symmetric aqueous redox-flow batteries. *ACS Energy Lett.* **1**, 976–980 (2016).
  135. Dieterich, V. et al. Estimating the cost of organic battery active materials: a case study on anthraquinone disulfonic acid. *Transl. Mater. Res.* **5**, 034001 (2018).
  136. Kwabi, D. G., Ji, Y. & Aziz, M. J. Electrolyte lifetime in aqueous organic redox flow batteries: a critical review. *Chem. Rev.* **120**, 6467–6489 (2020).
  137. Elgrishi, N. et al. A practical beginner’s guide to cyclic voltammetry. *J. Chem. Educ.* **95**, 197–206 (2018).
  138. Wang, H. et al. Redox flow batteries: how to determine electrochemical kinetic parameters. *ACS Nano* **14**, 2575–2584 (2020).
  139. Luo, J. et al. Unraveling pH dependent cycling stability of ferricyanide/ferrocyanide in redox flow batteries. *Nano Energy* **42**, 215–221 (2017).
  140. Yao, Y., Lei, J., Shi, Y., Ai, F. & Lu, Y.-C. Assessment methods and performance metrics for redox flow batteries. *Nat. Energy* **6**, 582–588 (2021).
  141. Zhang, J. et al. An all-aqueous redox flow battery with unprecedented energy density. *Energy Environ. Sci.* **11**, 2010–2015 (2018).
  142. Li, Z. & Lu, Y.-C. Polysulfide-based redox flow batteries with long life and low levelized cost enabled by charge-reinforced ion-selective membranes. *Nat. Energy* **6**, 517–528 (2021).
- Reports a charge-reinforced Nafion membrane to achieve low crossover of polysulfide species, along with demonstrating long-life and low-cost aqueous RFBs.**
143. Wu, M. et al. Extremely stable anthraquinone negolytes synthesized from common precursors. *Chem* **6**, 1432–1442 (2020).
  144. Machado, C. A. et al. Redox flow battery membranes: improving battery performance by leveraging structure–property relationships. *ACS Energy Lett.* **6**, 158–176 (2020).
  145. Lu, W. et al. Porous membranes in secondary battery technologies. *Chem. Soc. Rev.* **46**, 2199–2236 (2017).
  146. Doris, S. E. et al. Macromolecular design strategies for preventing active-material crossover in non-aqueous all-organic redox-flow batteries. *Angew. Chem. Int. Ed.* **129**, 1617–1621 (2017).
  147. Liu, W., Lu, W., Zhang, H. & Li, X. Aqueous flow batteries: research and development. *Chem. Eur. J.* **25**, 1649–1664 (2019).
  148. Goulet, M.-A. & Aziz, M. J. Flow battery molecular reactant stability determined by symmetric cell cycling methods. *J. Electrochem. Soc.* **165**, A1466–A1477 (2018).
  149. Wu, W., Luo, J., Wang, F., Yuan, B. & Liu, T. L. A self-trapping, bipolar viologen bromide electrolyte for redox flow batteries. *ACS Energy Lett.* **6**, 2891–2897 (2021).
  150. Zhao, E. W. et al. In situ NMR metrology reveals reaction mechanisms in redox flow batteries. *Nature* **579**, 224–228 (2020).
- One of the first demonstrations of in situ NMR spectroscopy to study the detailed mechanism underlying the redox reaction of organic molecules in RFBs.**
151. Wong, A. A., Rubinstein, S. M. & Aziz, M. J. Direct visualization of electrochemical reactions and heterogeneous transport within porous electrodes in operando by fluorescence microscopy. *Cell Rep. Phys. Sci.* **2**, 100388 (2021).
  152. Zang, X. et al. Monitoring the state-of-charge of a vanadium redox flow battery with the acoustic attenuation coefficient: an in operando noninvasive method. *Small Methods* **3**, 1900494 (2019).
  153. Sevov, C. S. et al. Physical organic approach to persistent, cyclable, low-potential electrolytes for flow battery applications. *J. Am. Chem. Soc.* **139**, 2924–2927 (2017).
  154. Yan, Y., Robinson, S. G., Sigman, M. S. & Sanford, M. S. Mechanism-based design of a high-potential catholyte enables a 3.2 V all-organic nonaqueous redox flow battery. *J. Am. Chem. Soc.* **141**, 15301–15306 (2019).

## Acknowledgements

C.Y. acknowledges the financial support from the Welch Foundation award F-1861, Camille Dreyfus Teacher-Scholar Awards and Sloan Research Fellowship. R.F. and W.W. acknowledge the financial support from the US Department of Energy, Office of Electricity (under contract no. 70247) and Energy Storage Materials Initiative, which is a Laboratory-Directed Research and Development project at Pacific Northwest National Laboratory (PNNL). PNNL is a multiprogramme national laboratory operated by Battelle for the US Department of Energy under contract DE-AC05-76RL01830.

## Author contributions

C.Y., W.W. and L.Z. contemplated the topic and structure of the Review. L.Z. and R.F. conducted the literature research. All authors contributed to the discussion of content and wrote and edited the manuscript.

## Competing interests

The authors declare no competing interests.

## Peer review information

*Nature Reviews Chemistry* thanks E. Izgorodina, R. Suman and the other, anonymous, reviewer(s) for their contribution to the peer review of this work.

## Publisher’s note

Springer Nature remains neutral with regard to jurisdictional claims in published maps and institutional affiliations.

© Springer Nature Limited 2022